Máster en Ingeniería Hidráulica y Medio Ambiente

Título del Trabajo Fin de Máster:

MAPEO DE RECURSOS EÓLICOS POR REDUCCIÓN DE ESCALA DE NCEP/NCAR REANALYSIS DATA 1 MEDIANTE EL MODELO DE MICROESCALA WAsP

Intensificación:

Recursos Hídricos

Autor:

BAYÓN i BARRACHINA, ARNAU

Directora:

Dra. LÓPEZ JIMÉNEZ, AMPARO

Fecha: *SEPTIEMBRE 2011*

Máster en Ingeniería Hidráulica y Medio Ambiente

Abstract (English):

The low accuracy of large-scale atmospheric models when assessing wind-energy resources and the scarcity of meteorological observations to use as boundary conditions for smaller-scale more-accurate models remark the need for downscaling techniques. Such techniques consist on using large-scale-model output as boundary conditions of smaller-scale models, so reaching significant data-refinement degrees. The final objective of this project is the development and subsequent validation of a downscaling tool to refine NCEP/NCAR Reanalysis Data 1 using microscale model WAsP.

For this, first, the WasP model is set up and wind climate maps of two regions of Europe are computed and validated at several points, at which meteorological observations are available. Those results, which constitute the long-term-prediction (climate) part of the project, are used as a part of the downscaling process. Furthermore, in order to assess their reliability, such results are also compared to the same wind map computation carried out by other authors before.

On the other hand, the short-term-prediction (meteorological) part of the project consists on the following: after downloading NCEP/NCAR Reanalysis Data 1 and deciding the operations to perform on them and on the afore-mentioned WAsP results, a MatLab routine is written to automatize the process. The downscaling technique proposed consists on extrapolating the wind climate at Point B out of meteorological observations from Point A using WAsP. Then, out of time-marching NCEP/NCAR Reanalysis Data 1 wind velocity profiles and other relevant data, online refined profiles of wind velocity and direction are obtained, which can be used for wind energy short-term predictions.

In order to assess the accuracy of the described tool, data of two episodes of 48h are downscaled and compared to observed meteorological data at two points of Europe, namely: Wideûmont (Belgium) and Carcaixent (Valencia). A sensitivity analysis is performed on the results, which demonstrates the effect of atmospheric stability, terrain-roughness estimations and other factors exert on the results.

Keywords:

Wind-energy, Downscaling, WAsP, NCEP/NCAR Reanalysis Data.

UNIVERSITAT POLITÈCNICA DE VALÈNCIA

Máster en Ingeniería Hidráulica y Medio Ambiente

Resum (Català):

La baixa precisió dels models atmosfèrics de gran escala per a avaluar els recursos eòlics i la manca d'observacions meteorològiques per a utilitzar com a condicions de contorn per a models d'escala menor de major precisió ressalten la necessitat de les tècniques de reducció d'escala. Aquestes tècniques consisteixen en utilitzar valors d'eixida de models de gran escala com a condicions de contorn de models d'escala menor, assolint així graus de refinament significatius. L'objectiu final d'aquest projecte és el desenvolupament i subseqüent validació d'una eina de reducció d'escala per a refinar dades del model NCEP/NCAR Reanalysis Data 1 utilitzant el model de micro-escala WAsP.

Per a això, el model WAsP és configurat i mapes eòlics de dues regions d'Europa són calculats i validats a diferents punts, per als quals es disposa d'observacions meteorològiques. Aquestos resultats, que constitueixen la part de prediccions a llarg termini (climàtiques) del projecte, són utilitzats com a part del procés de reducció d'escala. A més, a fi d'avaluar la seua fiabilitat, els esmentats resultats són comparats també al mateix càlcul de mapes eòlics efectuat per altres autors anteriorment.

D'altra banda, la part de predicció a curt termini (meteorològica) del projecte consisteix en el següent: rere descarregar les dades del model de reanàlisi del NCEP/NCAR i decidir les operacions a realitzar sobre aquestes i sobre els esmentats resultats de WAsP, una rutina de MatLab s'escriu per a automatitzar el procés. La tècnica de reducció d'escala proposada consisteix en extrapolar el clima eòlic a un Punt B a partir d'observacions meteorològiques d'un punt A utilitzant WAsP. Aleshores, a partir de sèries temporals del model NCEP/NCAR Reanalysis, perfils de velocitat de vent i altres dades rellevants, s'obtenen perfils refinats de velocitat i direcció de vent, els quals poden ser utilitzats per a predicció de producció d'energia eòlica a curt termini.

A fi d'avaluar la precisió de l'eina descrita, dades de dos episodis de 48h són reduïts d'escala i comparats a dades meteorològiques observades en dos punts d'Europa, a saber: Wideûmont (Bèlgica) i Carcaixent (València). Una anàlisi de sensibilitat s'efectua sobre els resultats, la qual demostra l'efecte de l'estabilitat atmosfèrica, les estimacions de rugositat del terreny i altres factors exerceixen sobre els resultats.

Keywords:

Energia eòlica, Reducció d'Escala, WAsP, NCEP/NCAR Reanàlisi.

UNIVERSITAT POLITÈCNICA DE VALÈNCIA

Máster en Ingeniería Hidráulica y Medio Ambiente

Resumen (Castellano):

La baja precisión de los modelos atmosféricos de gran escala para evaluar los recursos eólicos y la falta de observaciones meteorológicas para utilizar como condiciones de contorno para modelos de escala menor de mayor precisión resaltan la necesidad de las técnicas de reducción de escala. Estas técnicas consisten en utilizar valores de salida de modelos de gran escala como condiciones de contorno de modelos de escala menor, alcanzando así grados de refinamiento significativos. El objetivo final de este proyecto es el desarrollo y posterior validación de una herramienta de reducción de escala para refinar datos del modelo NCEP/NCAR Reanalysis Data 1 utilizando el modelo de microescala WAsP.

Para ello, el modelo WAsP es configurado y mapas eólicos de dos regiones de Europa son calculados y validados en diferentes puntos, para los que se dispone de observaciones meteorológicas. Estos resultados, que constituyen la parte de predicciones a largo plazo (climáticas) del proyecto, son utilizados como parte del proceso de reducción de escala. Además, a fin de evaluar su fiabilidad, los susodichos resultados son comparados también al mismo cálculo de mapas eólicos efectuado por otros autores anteriormente.

Por otro lado, la parte de predicción a corto plazo (meteorológica) del proyecto consiste en lo siguiente: tras descargar los datos del modelo de reanálisis del NCEP/NCAR y decidir las operaciones de realizar sobre éstos y sobre los susodichos resultados de WAsP, una rutina de MatLab se escribe para automatizar el proceso. La técnica de reducción de escala propuesta consiste en extrapolar el clima eólico en un Punto B a partir de observaciones meteorológicas de un Punto A mediante WAsP. Entonces, a partir de series temporales del modelo NCEP/NCAR Reanalysis, perfiles de velocidad de viento y otros datos relevantes, se obtienen perfiles refinados de velocidad y dirección de viento, los cuales pueden ser utilizados para predicción de producción de energía eólica a corto plazo.

A fin de evaluar la precisión de la herramienta descrita, datos de dos episodios de 48h son reducidos de escala y comparados a datos meteorológicos observados en dos puntos de Europa, a saber: Wideûmont (Bélgica) y Carcaixent (Valencia). Un análisis de sensibilidad se efectúa sobre los resultados, el cual demuestra el efecto que la estabilidad atmosférica, las estimaciones de rugosidad del terreno y otros factores ejercen sobre los resultados.

Keywords:

Energia eólica, Reducción de Escala, WAsP, NCEP/NCAR Reanálisis.

Acknowledgments

Vull agrair a totes les persones que han fet possible aquest projecte, tant al món acadèmic, com al personal. A Amparo, per la seua dedicació i paciència, a Nacho, Mar, Ester, Alberto y Guille per no tirar-me per la finestra quan els done la tabarra i a la família, amics i amigues per ajudar-me a mantenir el trellat gràcies al contacte amb el món no-acadèmic en general.

I also would like to thank the supervisors of this project at the VKI[1]: Prof. van Beeck for his wise advice and his always nice and encouraging spirit, especially in those moments when nothing works and you wonder what the point of your work is and even consider throwing your laptop through the window. Dank u wel! I also would like to thank Domingo for his support and advice, even not being in Belgium a part of the year. ¡Muchas gracias!

Of course, my most sincere thanks to my mates of the VKI in 2010/2011 in general: to the "Hungarian Mafia", to José Pedro and César, a.k.a. my personal "IT guys", for the technical support throughout the year, to Alex for his constant impertinence, to the "Young Balkan Hope", to the Italians, who made us look a little bit less noisy in the study room and to all my other dearly beloved nerds. I, per descomptat, als becaris espanyols per fer-me gaudir de tantes bones estones, fent així la feina quotidiana una mica més lleugera.

<div align="right">

Arnau Bayón i Barrachina.
València, September 1st 2011.

</div>

---

[1]This project was partially carried out at the Von Karman Institute for Fluid Dynamics (Belgium) during my stage in 2010-2011 as a scholarship holder.

Contents

List of Figures

List of Tables

List of Symbols

Acronyms

ABL	Atmospheric Boundary Layer
ANN	Artificial Neural Network
BZ	Bessel-Zooming
CFD	Computational Fluid Dynamics
CORINE	Coordination of Information on the Environment
DEM	Digital Elevation Model
ECMWF	European Center for Medium-Range Weather Forecasts
EEA	European Environment Agency
EWA	European Wind Atlas
FR	Flux Routines
GIS	Geographical Information System
GUI	Graphic User Interface
HIRLAM	High Resolution Local Area Modelling
IBL	Internal Boundary Layer
KAMM	Karlsruhe Atmospheric Mesoscale Model
MERRA	Modern Era Retrospective-analysis for Research and Applications
NCEP	United States National Center for Environmental Prediction
NCAR	United States National Center for Atmospheric Research
NMC	United States National Meteorological Center
OWC	Observed Wind Climate
PWC	Predicted Wind Climate
RLS	Recursive Least Squares
RMSE	Root Mean Squared Error
RWC	Regional Wind Climate
USGS	United States Geological Survey
VKI	Von Karman Institute
WAsP	Wind Atlas Analysis and Application Program

Roman symbols

A	Weibull scale parameter	
B	arbitrary coefficients	
c	Bessel-function zero	
f	Coriolis parameter	
g	acceleration of gravity	m/s^2
G	geostrophic wind	
h	height	m
H	total height above the sea level	m
J	Bessel function	
K	arbitrary coefficient	
l	near-surface layer thickness	m
L	characteristic depth of orography perturbations	m
p	pressure	Pa
P	porosity	
q	Weibull shape parameter	
Q	gravity ratio	m
r	Earth radius	m
R	computational domain radius	m
t	time	s
T	temperature	K
u	wind velocity	m/s
U	wind velocity horizontal component (X–axis)	m/s
V	wind velocity horizontal component (Y–axis)	m/s
$\bar{x}$	distance to the obstacle	m
z	height above ground level	m

Greek symbols

β	wind direction	^{o}
γ	offset	
Γ	Gamma function	
Δ	perturbation	
ϵ	scale factor	
χ	flow potential	
κ	von Karman constant	
∇	divergence operator	
Φ	geopotential	m^2/s^2
ρ	density	kg/m^3

Sub- and Superscripts

$'$	maximum
$*$	characteristic lengthscale
$0j$	roughness length
0	standard
e	equatorial
g	geopotential
i	term of a series
j	term of a series
k	wind direction sector
n	order of the Bessel function
N	NCEP/NCAR Reanalysis Data 1
p	polar
τ	shear
$terr$	above terrain level
ref	reference
W	WAsP

Chapter 1

Introduction

Atmospheric flow is one of the most complex and challenging to describe in the field of Fluid Mechanics. Indeed, its study led to Edward Lorenz to postulate his Chaos Theory, in which he describes the so-called *deterministic chaos* as a system in which, despite the governing equations are well known, the number of involved degrees of freedom is so large that they are extremely sensible to initial conditions (i.e. the butterfly effect). For this reason, exact long term forecasting is not feasible. This applies to the atmospheric flow perfectly.

Nevertheless, different approaches exist in order to provide sufficiently reliable weather predictions, most of them based on numerical modeling. The main difference between such techniques is the scale which they work at, as a very wide range of scales coexist in the atmospheric flow, which is likely what makes its study so complex. Fig. 1.1 and 1.2 show different attempts to classify such scales both in space and time, although no exact thresholds can be established between them.
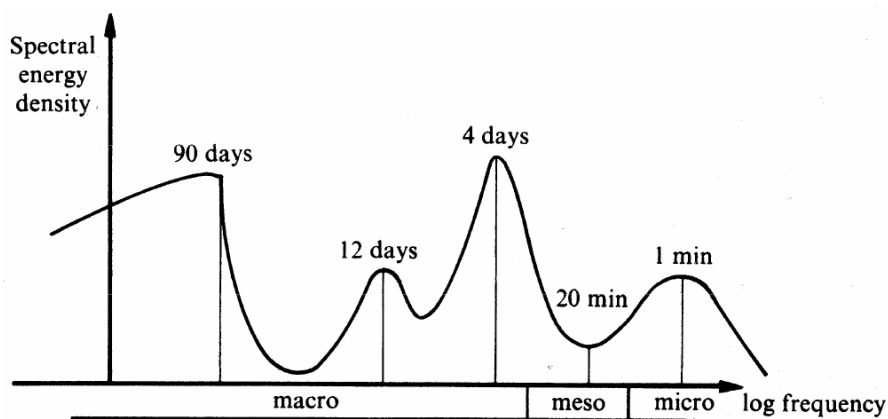
Figure 1.1: Frequency spectrum of the most relevant atmospheric turbulent flow processes and their characteristic times.

Figure 1.2: Atmospheric time and spatial scales approximate classification ([20]).

Such a large difference between coexisting-phenomena scales makes that, when it comes to assessing wind energy resources over a given area, no mathematical model (either macro-, meso- nor microscale) provides a perfect definitive solution. As it is discussed in the following paragraphs, all of the approaches have pros and contras.

Microscale models of atmospheric flow are the most widely used. Nevertheless, as stated in [1], they require data from a dense coverage of meteorological stations as input, which is often not available. In some cases, there are no available data at

2

all. Smaller-scale processes can be modeled by means of CFD techniques, but the large Reynolds numbers and the high number of degrees of freedom restrict this approach to very small scales (otherwise, computational costs become extremly high or simplifications excessively severe). For the above-mentioned reasons, in order to ensure a wind-energy-resources assessment system which can be applied at any point on Earth, at a suitable scale featuring every involved phenomenon and ensuring certain accuracy in the results, a different approach has to be carried out.

Mesoscale models , according to [2], provide currently a worldwide set of data on over-
all weather condition, but they cannot be used either to compare simulations with in-situ measured wind conditions nor to assess wind farm sites for power production purposes. This is due to the fact that small-scale orography and roughness features in the surroundings of points under study are not explicitly resolved by those models (results are grid-averaged). This leads to the so-called "false geographic precission", as two points relatively close to each other and same weather condition may fall in different grid boxes with quite different mean values. Therefore, despite mesoscale models can increase their horizontal resolution down to $2km$, the mismatch between numerical weather prediction (henceforth, NWP) grid-averaged output and actual conditions can only be reduced only to a certain extent ([3]).

Therefore, *downscaling techniques*, which combine the advantages of both micro- and mesoscale models (i.e. high accuracy and data availability, respectively), become necessary. Such techniques, which consist essentially of using large-scale-model results as boundary conditions to run smaller-scale models, are truly the leitmotiv of the present research project. A discussion on the state of the art of the different downscaling methods types is carried out in Sec. 1.2.

1.1 Project goals

The overall scope of this project is estimating wind-energy resources over the terrain by means of mathematical modeling. In a more specific field, the goal of this thesis is developing a downscaling tool in order to use mesoscale-model results as input of a microscale model (i.e. downscaling). In this case, the mesoscale data used are the *NCEP/NCAR Reanalysis Data 1*: a worldwide dataset obtained by means of reanalysing atmospheric data (i.e. using present data after their assimilation to reprocess past-time values and to infer in atmosphere evolution). This dataset is freely provided by the U.S. *National Center for Environmental Prediction* (NCEP) and the U.S. *National Center for Atmospheric Research* (NCAR), in [18].

The microscale model used is *WAsP* (*Wind Atlas Analysis and Application Program*), a widely-used commercial code developed by the *Risø National Laboratory* of Denmark. Further discussion on the models' characteristics is carried out in Chap. 2.

The downscaling process proposed is automatized thanks to a *MatLab* routine, which is programmed in the context of this project. How this is done is also discussed in Chap. 2. The downscaling tool is tested and validated using meteorological station observations at two points of Europe, whose results are discussed in Chap. 3.

Besides the development of the afore-mentioned downscaling tool, wind maps of Belgium and the Valencian Country, Catalonia and the Balearic Islands are computed as well by means of *WAsP* exclusively. This preliminary task is carried out in order to become familiar with the use of *WAsP* and to assess its features, accuracy, etc. although, out of the *WAsP* setup to compute a the afore-mentioned wind atlas, some results are subsequently used as input of the downscaling tool, as discussed below. Average wind condition is assessed at five points in Belgium and two points in the Valencian Country, at which there are meteorological stations and whose observations can be compared to the *WAsP* results (see Sec. 3.1).

1.2 Downscaling

Downscaling techniques in mathematical modeling are a particular case of *nesting* which consist in taking output data from large-scale models and adding information at scales smaller than the original grid resolution. Their final purpose is refining the results from the large-scale model, in which local features are not explicitly resolved, by means of using a smaller-scale model. Their main assets can be summarized in two:

- No in-situ time-series are required and microscale models can be therefore applied worldwide in a systematic way, as long as consistent data are provided by the larger-scale model.

- Macro- and mesoscale model can be used not only to study mid- and long-term trends, climate change and global-scale phenomena, but also to asses wind-energy resources.

Downscaling methods can be split into three general types or approaches: statistical, physical and hybrid (or physical-statistical). Such methods are discussed on Sec. 1.2.1, 1.2.2 and 1.2.3, respectively.
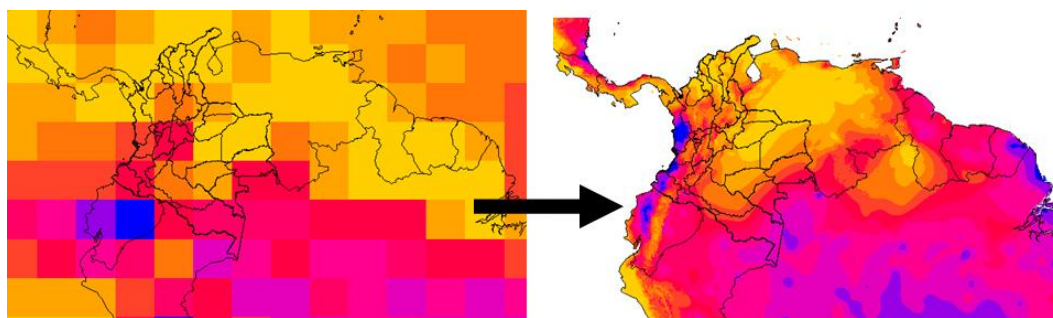
Figure 1.3: Example of geospatial data refined by downscaling.

1.2.1 Statistical methods

As defined by [4], statistical downscaling methods in their pure form are "a try to find the relationships between a wealth of explanatory variables (predictors), including NWP results and/or online measured power data, usually employing recursive techniques. Often, *black-box* models like advanced Recursive Least Squares (RLS) or Artificial Neural Nerworks (ANN) are used. Statistical models can be used at any stage of the modelling and often combine various or even all of the steps into one, which is an advantage in some cases". In other words, the relationship between variables is figured out in a non-deterministic way, i.e. misregarding the physical laws which govern the phenomenon under study.

Statistical downscaling methods are therefore able to provide good results with low computational resources consumption, as the equations used tend to be simpler than those used in physical downscaling. In connexion with this, [3] claims that statistical downscaling methods yield accurate results when wind condition is predicted at sites where a large number of observations is available, whereas points far away from meteorological stations require a physical downscaling approach, as the lack of information can be replaced by physically-based equations.

According to [4] and in connection with the chaotic behavior of the atmosphere, "models not using NWP-output data have a quite good accuracy for the first few hours, but are generally useless for longer prediction horizons (except in very special cases of thermally driven winds with a very high pattern of daily recurrence). On the other hand, models independent of online data, such as the Danish model *Zephyr*, can bring results for a new farm from day 1, while the advanced statistical models need older data to learn the proper parametrizations. However, this is bought with a reduced accuracy for rather short horizons".

1.2.2 Physical methods

The second type of downscaling methods are the so-called physical, dynamic or deterministic methods, which are defined by [4] as a physical or deterministic approach, based on our knowledge on fluid mechanics and physics of the atmosphere, to obtain the best estimate of the observed wind conditions instead of using model output statistics. Examples of this approach are the *2L-model* and the *Flux Routines*.

2L-model Most of the models used, such as the *2L-model* ([5]), are based on the assumption that sub-grid-scale wind velocity perturbations are esentially produced by successive changes of surface roughness. Such variations are modeled by means of conventional boundary layer theory. The *2L-model* comprises a surface logarithmic layer and an Ekman-layer (turbulent flow resulting from the interaction of a pressure gradient, the Coriolis force and the surface drag). "In the surface layer vertical wind speed transformations are done using the logarithmic wind speed profile. In the Ekman-layer geotrophic resistance laws are applied" ([5]). According to the same source, the model developed by their team is better suited when dealing with many consecutive roughness changes (implements direction-variable roughness lengths) than the methods based on an Internal Boundary Layer (IBL) approach, such as *WAsP* (see further sections), which require a well defined sequence of roughness changes, leading to major roughness zone simplifications. Indeed, this model is already been successfully used by [5] to downscale *HIRLAM* (*High Resolution Local Area Modelling*) model output data, significatively improving its results, except for coastal and off-shore locations. Nevertheless, *WAsP* can model topography-driven flow, while the *2L-model* cannot (it has to be forced by the input mesoscale model), so it has to be applied only to smaller scales.

Flux-Rutines Also more complex microscale models have been used for atmospheric flow model downscaling purposes. E.g. [3] used *Flux Routines* (*FR*) with mesoscale model output (or synoptic observations) at a single level plus cloud cover data as input. The *FR* are composed of parametrizations concerning the radiation components and the surface fluxes, while the aerodynamic resistance is determined with Monin-Obukhov theory. However, due to their complexity, they are out of the scope of this study.

1.2.3 Physical–statistical methods

A third family of downscaling methods can be defined, the so-called physical–statistical or hybrid methods which, according to [4], turn out to be the most successful ones. They normally are *grey-box* models as, although being essentially statistically-based, some knowledge on the atmosphere physical behavior is used to adapt the models to the

case under study. In agreement with this, [3] claims that downscaling wind speed techniques should always combine both phyisical and statistical methods in order to achieve the best possible results.

KAMM/WAsP A good example is exposed in [1], in which *Karlsruhe Atmospheric Mesoscale Model* (*KAMM*) –a 3-dimensional, non-hydrostatic atmospheric mesoscale model– results are refined by downscaling using the *WAsP* concept of the generalized wind climate of a region, i.e. "the wind climate for standard conditions given by flat terrain of uniform roughness" ([2]). Hence, generalized wind climate shows the wind condition variation due exclusively to mesoscale flow features, removing the local orography and roughness effects. The *KAMM* model uses *NCEP/NCAR Reanalysis Data 1*, which are analysed to obtain wind statistics for a given site ([6]). The results, thanks to a site environment description, are "cleaned" of local effects, so obtaining a generalized wind climate or wind atlas (see further sections), which is the natural *WAsP* input data format. The same authors found out that, to a certain extent, the final results obtained by this procedure are fairly independent of the grid resolution of the mesoscale model, which is encouraging as proves how useful downscaling methods can be.

After an intense bibliographic search, syntetized in the previous paragraphs, the model *WAsP* turns out to be the most appropriate model: not only yields generally the best results, but it also is backed up by its wide use among the wind engineering community. The downsacaling method proposed by this text belong to the latter cathegory exposed (i.e. physiscal–statistical methods): on the one hand, this project uses mostly statistical tools to combine data from mesoscale models and *WAsP* output data (i.e. the "statistical" part of the process). On the other hand, the use of *WAsP* output data and the *NCEP/NCAR Reanalysis Data 1* involves the "physical" part of the downscaling process, since they come from mostly-deterministic models.

Chapter 2

Materials and methods

This section deals with the two models involved in the proposed downscaling process (the *NCEP/NCAR Reanalysis Project* and *WAsP*, Sec. 2.1 and 2.2, respectively) and the two main parts in which the present project is split, namely:

- Obtention of a wind atlas of Belgium and the Valencian Country, Catalonia and the Balearic Islands using microscale model *WAsP* (Sec. 2.3).

- Development and validation of a downscaling tool using *NCEP/NCAR Reanalysis Data 1* and *WAsP* oriented to the wind-energy resources assesment (Sec. 2.4).

2.1   NCEP/NCAR Reanalysis

As stated in Chap. 1, the *NCEP/NCAR Reanalysis Data 1* is the dataset used as large-scale model data in the context of this project. Such data, available at [18], consist of a continuously updated gridded dataset, which provides a wealth of atmospheric variables (air temperature, humidity, pressure, wind velocity, etc.) consistent in time and space at respective resolutions down to $6h$ in time and 2.5^o in horizontal coordinates[1]. Its vertical resolution is defined by 17 pressure levels (as many atmospheric models, vertical coordinates are defined by pressure levels instead of geometric heights, see 2.4.2). The *NCEP/NCAR Reanalysis Data 1* time coverage ranges from 1948 to the present whereas the spatial one is worldwide.

The *NCEP/NCAR Reanalysis Project*, a state-of-the-art research-oriented official program resulting from the collaboration of the U.S. *National Center for Environmental Prediction* (NCEP), the U.S. *National Center for Atmospheric Research* (NCAR) and plenty of of institutions from dezens of countries, is based on a powerful atmospheric numerical model of several modules. The main ones, whose functions are briefly discussed in Sec. 2.1.1, 2.1.2 and 2.1.3 (for more in-depth details, see [18]), are the following:

---

[1]In the Y-axis (N-S), this is, approximately, $160km$. In X-axis (W-E), 2.5^o is, approximately, $285km$ and $210km$ at Belgian and Valencian latitudes, respectively.

– Data decoder and quality control,

– Data assimilation and monitoring module,

– Archive module.

2.1.1 Data harvest

All raw meteorological data to feed the numerical model are obtained out of field measurements harvested by means of land-surface stations, ships, rawinsondes, pibals, aircrafts, satellites and other sources. Such data are obviously provided at very different time and spatial resolutions, since their distribution in space is highly irregular and sources of data change throughout the years. In-depth details on the different time-series origin are provided by [18].

2.1.2 Data assimilation

Once data are harvested and decoded, a subsequent analysis of these measurements in order to provide a consistent set of values relative to the state of the atmosphere is carried out: it is the so-called assimilation. This process in this case consists on a spectral statistical interpolation based on a three-dimensional variatonal analysis scheme, which is carried out thanks to the *T62/28 NCEP Global Spectral Model*. Such model works at different spatial and time resolutions. In the horizontal coordinate, the mesh size spans from $125km$ to $210km$ (although data are provided by the final model output, the *NCEP/NCAR Reanalysis Data 1*, in a 2.5^o-resolution grid), whereas in the vertical axis, the model is resolved at 28 pressure levels, although only 17 are provided by the final model output.

In order to ensure that the atmospheric boundary layer (henceforth, ABL) is properly resolved, despite the final model output does not provide data at such low gridpoints, the *T62/28 NCEP Global Spectral Model* grid reaches points down to $3 - 5hPa$ from the terrain surface. As regards time, the model works with different resolutions, which reach $3h$-timesteps, although the final model output does not provide values below a timestep of $6h$. All of these measures reduce significantly the errors inherent to every interpolation process with respect to older statistical analysis.

The assimilation process, which also detects wrong measurements or other sources of unexplainable meteorological jumps, represents the central module of the *NCEP/N-CAR Reanalysis Project* numerical model and it has suffered very little changes since the project started back in the 1990s[2]. Note that the use of a quasi-frozen analysis system like this one avoids the bias introduced by model changes, as shows Fig. 2.1.2.

---

[2]Variations in the *NCEP/NCAR Reanalysis Data 1* assimilation system were eventually introduced due to the addition or removal of meteorological-observation sources in the different stages of the project.

Tv 1000 mb Pacific 30N-30S 120E-90W
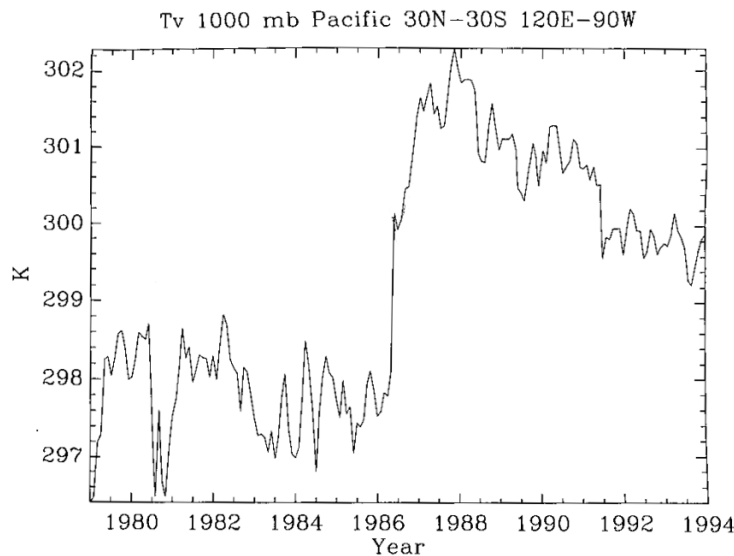
Figure 2.1: Example of the effects on NCEP/NCAR Reanalysis Data 1 temperature values after assimilation due to the bias introduced by a model switch in a gridpoint in the Pacific Ocean ([18]).

2.1.3 Data reanalysis

As in many of the new-generation models, a state-of-the-art reanalysis is also performed on the *NCEP/NCAR Reanalysis Data 1* after their assimilation. This process consists on recomputing past-time values using online information, in order to detect trends and patterns and to differentiate the statistical annual variability of the atmospheric properties from those variations due to the mid- and long-term climate change.

Therefore, the reanalysis process should resolve a wealth of mid- and long-term atmospheric features, such as the turbulent transport of greenhouse gases between atmospheric layers. Nevertheless, the storage and computational requirements for this far exceeded what originally the project could afford. For this reason, simple monthly reanalysis were carried out at first, which left a door open to performing shorter reanalysis in the future.

2.1.4 Data selection

As the *NCEP/NCAR Reanalysis Data 1* provides information on a wealth of meteorological variables, a paramount task is determining which of those data happen to be relevant for this project's purpose. Downloading just these data in a selective way is possible thanks to the data-subset extraction tool available in [18]. In this case, according to the reasons stated in Sec. 2.4, the relevant data are the following:

– wind velocity in X, i.e. East-to-West direction (U),

– wind velocity in Y, i.e. South-to-North direction (V),

– geopotential height[3] (z_g),

at a single gridpoint, at the 17 pressure levels available, namely: $1000mb$, $925mb$, $850mb$, $700mb$, $600mb$, $500mb$, $400mb$, $300mb$, $250mb$, $200mb$, $150mb$, $100mb$, $70mb$, $50mb$, $30mb$, $20mb$, $10mb$, and at a $4x/day$ time resulution ($6h$ timestep).

Obviously, not every pressure level's wind condition is relevant in order to determine the near-surface wind resources (e.g. pressure level $10mB$ is generally dezens of kilometers above the ground level, in the mid-stratosphere, and so its weather has nothing to do with the low-troposphere one). For this reason, which pressure levels whether must be taken into account or not is a paramount decision, but this topic will be discussed below, in Sec. 2.4.

---

[3]The geopotential height is a "gravity-adjusted height" which is widely used in numerical weather prediction (NWP) as it allows neglecting centrifugal forces and air density effects, which are complex to model. Thanks to that discussed on Sec. 2.4.2 on Pag. 32, geopotential heights can be easily converted to geometric heights.
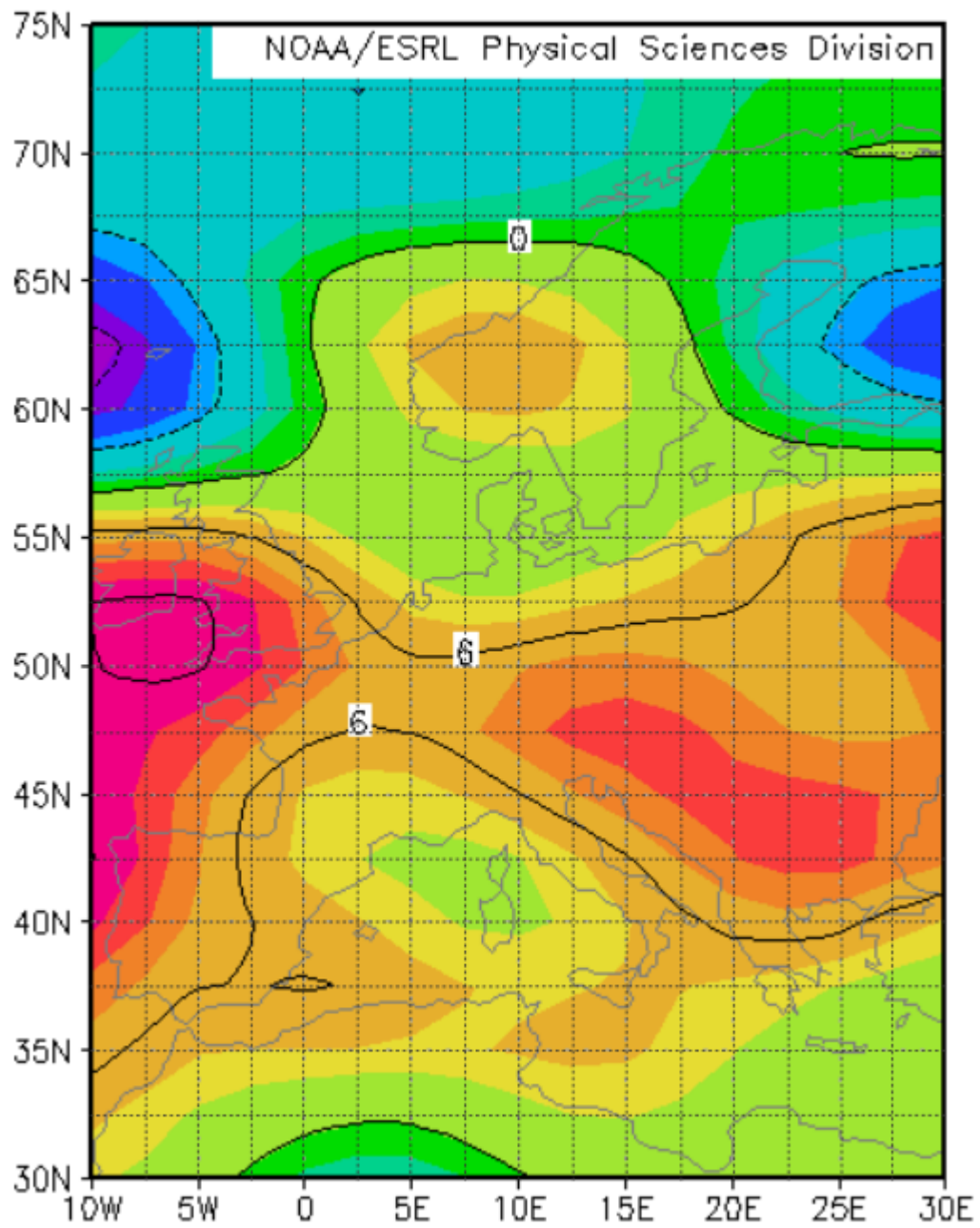
Figure 2.2: NCEP/NCAR Reanalysis Data 1 example; horizontal velocity (U) at pressure level of $850mb$, at 0h of December 1st 1985; positive direction: West to East ([18]).

2.2 WAsP

The already-mentioned *WAsP* (*Wind Atlas Analysis and Application Program*) is a commercial software developed by the *Risø National Laboratory* (Denmark) and it is widely used to predict wind climate and wind-energy production. This program is nothing but an application of the Wind Atlas methodology, whose details are explained in depth in [7] and summarized in [1]. The main advantatge of *WAsP* is that, thanks to the use of linearized equations instead of the Navier-Stokes Equations to resolve the atmospheric flow, the model can be run in any personal computer (powerful computers are not necessary and still computational times are acceptable). It is worth remarking that, despite its severe simplifications, the *WAsP* setting up is not trivial (as it is explained below) and this model yields quite good results, being thus so widely used.

2.2.1 Model

This section briefly deals with the basics of the *WAsP* model, i.e. the Wind Atlas methodology ([7]) relative to wind climate assessment. Note that further computations (such as estimating annual energy production) can be carried out using this software, but data on specific wind-turbines characteristics, distribution over the terrain, etc. have to be provided. Since this thesis is oriented to the study of the atmospheric flow, such considerations are out of the scope of this project and so they are not discussed in this section.

Weibull distribution

As many wind prediction models, *WAsP* is based on the hypotesis that wind speed data can be approached in statistical terms by the Weibull distribution, a continuous probability distribution, which is widely accepted among the wind-engineering community. Its probaility density is given by the following function:

$$f(u) = \frac{q}{A} \left(\frac{u}{A}\right)^{q-1} exp\left(-\left(\frac{u}{A}\right)^q\right) \qquad \text{(Weibull distribution)}$$

where A is the scale parameter and q the shape parameter. The Weibull distribution is related to other probabilistic distribution, e.g. the exponential distribution (particular case $q = 1$) or the Rayleigh distribution (particular case $q = 2$).

As velocity distributions at a given point are denoted by their Weibull function in *WAsP*, in order to be able to represent wind velocities at several points as a wind-velocity profile, the mean value insted of the complete statistical distribution has to be used, although it means a simplification of information. The main advantage is that,

besides obtaining a scalar to represent wind profiles, it is a very intuitive variable in order to compare diffferent wind conditions. The mean value of a Weibull distribution can be obtained thanks to a well-known function of differential calculus, the Gamma function (Γ), as follows:

$$E(u) = A \cdot \Gamma \left(1 + \frac{1}{q}\right) \tag{2.1}$$
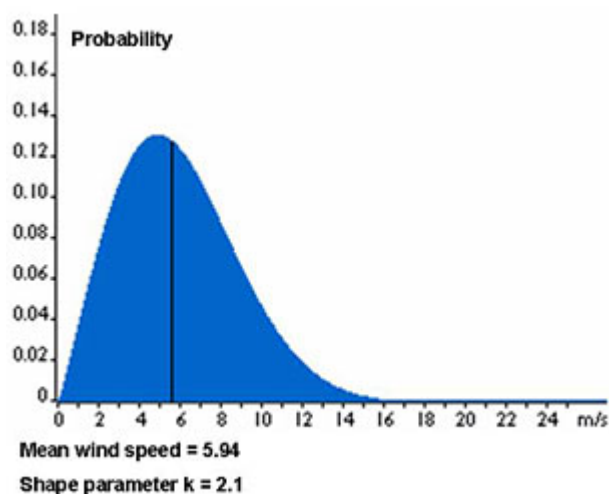
Figure 2.3: Example of a Weibull distrbution.

Wind rose

The windrose (i.e. sectorwise representation of frequencies of wind direction) is represented in *WAsP* split in sectors (hence, the wind rose can be seen as a circular histogram). Thus, winds are characterized by thir velocity (represented by the Weibull parameters) and a sector according to their direction. By default, in *WAsP* sectors range clockwise from 1 to 12, covering 30° each and being sector 1 the North.

Regional wind climate

WAsP most basic assumption is, according to [1], that for a specific microscale area, the overall wind conditions (i.e. the geostrophic wind climate) change so slowly that the wind climate can be extrapolated from a meteorological station (*Point A*) to any point of the region (*Point B*) just taking into account the local effects at both sites.

The so-called *site effects* are surrounding obstacles and roughness and orography of the terrain in the vicinity of the points under study and are taken into account as follows: the observed wind climate (henceforth, OWC) at *Point A* is affected by the particularities of the surrounding topography, the terrain roughness and the shelter produced by close obstacles. In order to extrapolate this wind climate to *Point B*, the wind conditions in *Point A* have to be "cleaned" of site effects, resulting the so-called regional wind climate (henceforth, RWC). This generalized wind climate, defined by [2] as "the wind climate for standard conditions[4] given by flat terrain of uniform roughness", is considered extrapolable. Therefore, to estimate the wind resource at *Point B*, it only has to be affected by *Point B* site effects (see Fig. 2.4).

Figure 2.4: Scheme of the Wind Atlas methodology ([7]).

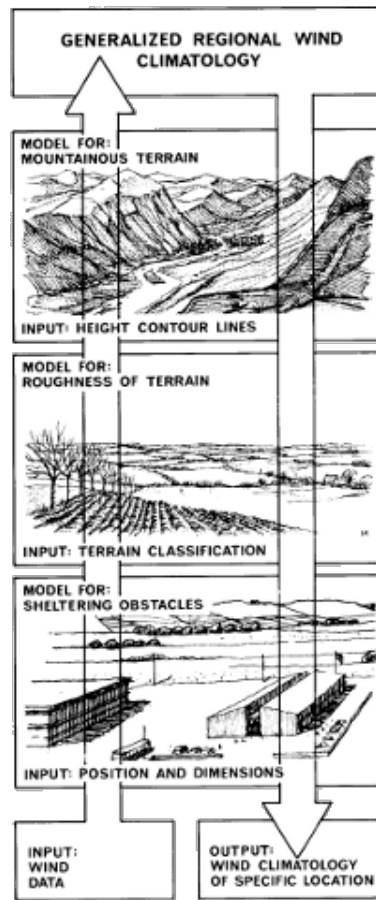[4]These standard conditions (RWC) are denoted by sector–wise Weibull distributions (given by the Weibull parameters: A and k) at different heights (height classes) and in turn in different uniform terrain roughnesses (roughness classes). By default, such classes are 5 and 4, respectively. Points between two classes must be interpolated.

Orography

In *WAsP*, orography is resolved up to horizontal scales of tens of kilometres by means of the *Bessel-Zooming model* (BZ-model), which assumes a potential-flow approach (see Eq. 2.2). This model resolves the flow at every point of a polar-zooming grid around the points under study, i.e. *Point A* or *Point B*, using the previous section nomenclature (see Fig. 2.5).
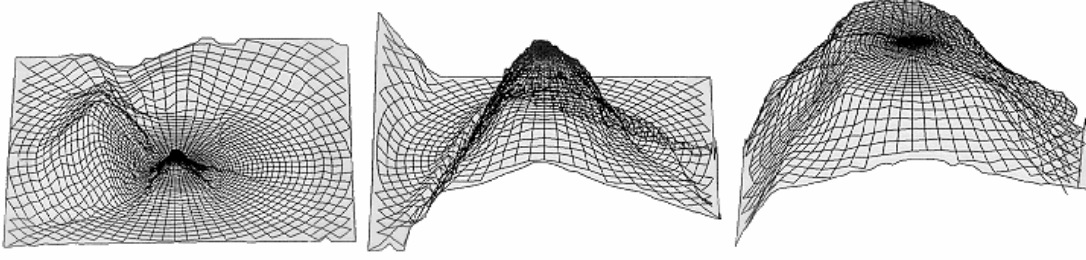
Figure 2.5: Polar-zooming grid around a point under study (BZ-model).

This allows higher resolutions in the vicinity of the afore-mentioned points (down to $2m$ for a domain radius of $R = 10km$ and cell-to-cell growing rate of 1.06). The relationship between flow potential and velocity is expressed as follows:

$$\vec{u} = \nabla\chi \tag{2.2}$$

where $\vec{u} = (u, v, w)$ is the three-dimensional velocity perturbation vector and χ the flow potential, which can be expressed in polar coordinates as the sum of the following terms:

$$\chi_j = K_{nj}J_n\left(c_j^n\frac{r}{R}\right)exp(in\o)exp\left(-c_j^n\frac{z}{R}\right) \tag{2.3}$$

where K_{nj} are arbitrary coefficients (which depend on the boundary conditions, see [7]), J_n the nth-order Bessel function, r the polar coordinate, $\o$ the azimuth, z the height and c_j^n the ith zero of J_n. Nevertheless, potencial flow couples pressure gradients and advection of momentum, neglecting turbulent momentum transfer. This assumption cannot be done at the near-surface layer, where stability cannot be warranted and whose thickness can be estimated as follows:

$$l_j = 0.3z_{0j} \left(\frac{L_j}{z_{0j}} \right)^{0.67} \tag{2.4}$$

where z_{0j} is the surface roughness lenght and $L_j = \frac{R}{c_j^1}$, which can be interpreted as both the horizontal scale and the characteristic depth in which perturbations due to orography penetrate. In the particular case of homogeneus-roughness, it can be assumed that: $z_{0j} = z_0$; in other cases, [7] explains the approach to follow. Hence, for scales smaller than l_j, perturbations are computed applying the following correction to the flow potential:

$$\frac{\Delta \vec{u}_j(z)}{|u_0(z)|} = \frac{|u_0(L_j)|^2}{|u_0(z_j')|} \nabla \chi \tag{2.5}$$

where $u_0(z)$ is the non-perturbed velocity profile and $z_j' = max(z, l_j)$ (maximum of the height and the thickness of the the near-surface layer at which stability cannot be warranted.

Obstacles

Figure 2.6: Downstream obstacle shelter effects.

Obstacles in the vicinity of the point under study may play a paramount role in the assessment of wind climates. The magnitude of this effect depends on the dimensions of the object, its orientation and the distance to the point under study.

The disturbance in the wind velocity vector due to the shelter produced by surrounding obstacles is modeled by *WAsP* under a two-dimensional semi-infinite obstacle approach, which extended to three-dimensional cases, as explained in [7]. This velocity deficit ($\tilde{u}$) is defined as the difference between the reference velocity –without the obstacle– and the actual velocity –with the obstacle– with respect to the former, multiplied by the distance to the obstacle. According to the model description in [7], this variable can be empirically reasonably-well approached by:

$$\tilde{u} = -\frac{\Delta \bar{u}(z)}{\bar{u}_{ref}(h)} \cdot \bar{x} = 9.75(1-P) \cdot \eta \cdot exp(-0.67\eta^{1.5}) \qquad (2.6)$$

where P is the porosity and $\eta = \frac{z}{h-d}(K\bar{x})^{-\frac{1}{n+2}}$ (h is the obstacle height, d the flow displacement height and $\bar{x} = \frac{x}{h-d}$; parameters K and n defined in [7]). It is worth remarking the importance of modeling obstacles shelter effects separately from roughness and topography, as obstacles produce generally flow separation, which violates the computational envelope of *WAsP*, which is based on the assumption of potential flow, as mentioned above.

Roughness

As regards roughness, another paramount assumption of *WAsP* is, according to [1], that this magnitude affects to the wind speed profiles in two different ways, namely: as uniform roughness, describing a logarithmic wind velocity profile, and as roughness changes, developing one or more internal boundary layers (henceforth, IBL).

Uniform roughness lenght

The wind profile is defined by the so-called geostrophic drag law, i.e. the relation between the surface friction velocity and the geostrophic wind (produced by synoptic pressure gradients), which is valid under homogeneity, stationarity and stability conditions and is defined as:

$$sin\alpha = -\frac{Bu_\tau}{\kappa G} \qquad \text{(Geostrophic drag law)}$$

where u_τ is the friction velocity, defined as:

$$u_\tau = \sqrt{\frac{|\tau_{z=0}|}{\rho}} \qquad \text{(Surface friction velocity)}$$

and α is the theoretical solid angle between the surface winds and the geostrophic wind (G), which can in turn be defined by means of the following expression:

$$G = \frac{u_\tau}{\kappa} \sqrt{\left(ln\left(\frac{u_\tau}{fz_0}\right) - A\right)^2 + B^2} \qquad \text{(Geostrophic wind)}$$

where f is the Coriolis parameter, z_0 is the roughness lenght, $\kappa = 0.4$ is the von Karman constant and A and B are empirical parameters. Such parameters are constant under atmospherical stability conditions. Although atmospherical instability is often neglected when it comes to wind energy (it mostly occurs associated to low wind speeds), *WAsP* does model it as small perturbations to a basic neutral state, taking into account surface temperature and heat flux (see [7] for further details).

Roughness changes

Roughness changes affect the friction velocity law, thus when they occur another approach is necessary. As discussed when comparing *2L-model* to *WAsP*, the latter models roughness lenght changes assuming that an internal boundary layer (IBL) is developed downstream every roughness lenght change. This phenomenon is sketched in Fig. 2.7.
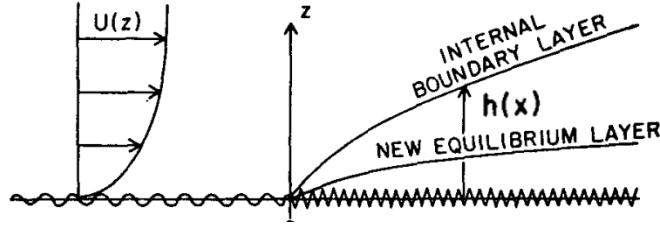
Figure 2.7: Development of an internal boundary layer due to roughness changes.

According to [7], the IBL maximum height (above it, no roughness change is felt) can be approached by the following empirical equation:

$$\frac{h'}{z_0'}\left(ln\frac{h'}{z_0'} - 1\right) = 0.9\frac{x}{z_0'} \qquad (2.7)$$

where $z_0' = max(z_{01}, z_{02})$ and x is the downstream distance. In order to compute the maximum approximate height at which IBLs can exert their effects, a roughness lenght of $z_0'(max) = 1.00m$ and a maximum fetch of $x(max) = 10km$ (maximum influence radius associated to high roughness values, according to [6]) are considered. This height turns out to be $h'(max) = 1440m$.

In order to describe the IBL profile, it can be easily demonstrated that the following relationship (resulting from matching of neutral wind profiles at the height h) is valid:

$$\frac{u_{\tau,02}}{u_{\tau,01}} = \frac{ln\left(\frac{h}{z_{01}}\right)}{ln\left(\frac{h}{z_{02}}\right)} \tag{2.8}$$

where the sub-index 01 and 02 mean upstream and downstream from the roughness change. Nevertheless, since the IBL perturbes the stable wind profile, an empirical approach has to be followed in order to define the wind velocity profiles within the IBL. Therefore, the following expression is implemented in *WAsP* to compute the effects of successive roughness changes on the wind velocity profile:

$$u(z) = \begin{cases} u' \frac{ln(z/z_{01})}{ln(c_1 h/z_{01})} & \text{if } z \geq c_1 h, \\ u'' + (u' - u'') \frac{ln(z/c_2 h)}{ln(c_1/c_2)} & \text{if } c_2 h \leq z \leq c_1 h, \\ u'' \frac{ln(z/z_{02})}{ln(c_2 h/z_{02})} & \text{if } z \leq c_2 h \end{cases} \tag{2.9}$$

where $u' = \frac{u_{\tau,1}}{\kappa} ln\left(\frac{c_1 h}{z_{01}}\right)$, $u'' = \frac{u_{\tau,2}}{\kappa} ln\left(\frac{c_2 h}{z_{02}}\right)$, $c_1 = 0.3$ and $c_2 = 0.09$. Thanks to Eq. 2.9 and 2.8, the IBL perturbation can be applied in sequence of successive roughness lenght changes.

2.2.2 Limitations

According to [6], *WAsP* computational domain must extend at least $R >= 10km$ away from the points under study. Large roughnes changes (e.g. a coast line) on the fetch of a frequent wind direction may require up to twice that value.

On the other hand, larger scales are not desirable as mesoscale effects, which are not taken into account by *WAsP* (e.g. Coriolis effect, thermally driven winds, etc.), may play an important role. Indeed, that is why mesoscale models are used as input in the context of downscaling.

[6] claims that typical annual energy prediction errors for wind turbines are about 10% in normal conditions, whereas in rugged terrain larger errors can be expected. Indeed, such regions are the weak point of *WAsP*.

Rugged terrain

As [1] reports, flow over rugged terrain, where separation is likely to occur –also called complex terrain– will in many cases not be modelled accurately. "To overcome this problem, two approaches are possible: the first is to develop correction algorithms to the existing simple model (by means of the Ruggedness Index –RiX–), the second, to develop a new model altogether" ([1]).

The RiX is defined by [11] as "the fraction of the surrounding terrain which is over a critical slope" on which flow attachment can no longer be ensured. The value 0.3 ([12]) is generally accepted as the slope threshold for flow separation to occur. The slope is computed on several radii out of the point under study as they intersect the elevation contour lines. But not always high RiX imply low accuracy. As stated by [11], "the sign and approximate magnitude of the preediction error due to orography is proportional to the difference in ruggedness between the predicted and reference sites".

For this reason, the RiX is used to correct *WAsP* results. Indeed, this method was successfully applied by [8] to the simulation of quite rugged terrain and compared to conventional CFD models based on a steady state time-independent solution for the wind and turbulence fields. In spite of their simplifications, such non-linear models still require enormous computational resources and no improvements were obtained by using them models with respect to *WAsP* ([8]).

Forested terrain

Another known issue of *WAsP* is the flow over forested areas, which represent an unfortunate type of terrain for wind turbines, mainly due to the high turbulence intensity and shear of the flow over the tree canopy. Nevertheless, wind turbines are becoming quite common in forested areas ([1], in agreement with [13]). The difficulty to predict the characteristics of such flows, as [13] reports, has led to a lack of consensus on how to model forestry in *WAsP* among the wind-energy scientific community and industry.

However, some directions are provided by [1]: forests represent a displacement height of the ground surface which, furthermore, "physically represents a porous surface and a porous surface in turn, has other consequences for the flow". The easiest –but also less accurate– approach to overcome this problem is to substract the displacement height (approximately, the trees canopy height) from the height at which the wind condition has to be estimated (e.g. the height of a meteorological station, a wind-turbine hub, etc.).
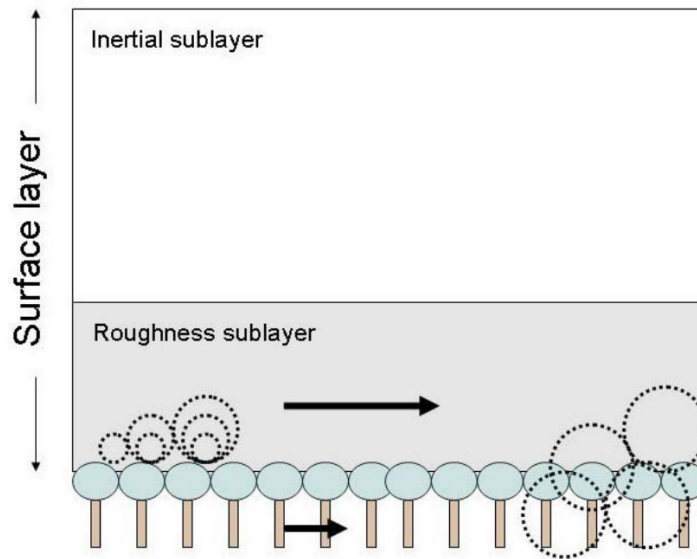
Figure 2.8: Development of secondary boundary layers over forested areas.

2.3 Wind Atlas

2.3.1 Description

As mentioned in Chap. 1, besides developing a suitable downscaling tool to use mesoscale-model output as microscale-model input, a preliminary task is carried out in the context of this project: computing a wind atlas of two zones of Europe using the microscale model *WAsP*. The reasons to do it are not only becoming familiar with the model and exploring its capabilities, but also setting it up for its further use as a part of the downscaling chain.

The zones under study are two: one in the Northern Europe (under the influence of the North Sea) and another one in the Southern Europe (influenced by the Mediterranean Sea). The European Wind Atlas ([7]) provides regional wind climate information obtained out of some meteorological stations in those zones, namely:

- **Northern Europe:**

  - *Florennes*
  - *Melsbroek*
  - *Middelkerke*
  - *Saint-Hubert*
  - *Spa*

- **Southern Europe:**

  – *Alacant*

  – *Barcelona*

  – *Girona*

  – *Mallorca*

  – *Menorca*

  – *València*

Using that information, after setting the model up, self- and cross-comparisons of wind-climate conditions are performed. A self-comparison consists on estimating the wind climate at the same point from which the RWC was obtained (wind data is "cleaned" of site effects and the same effects are applied again).

According to [7], provided that a good description of the site is done, self-prediction fairly matches the original meteorological data and so it is assumed in this case. A cross-comparison consists on computing wind resources using data from one point to extrapolate the wind conditions to another one (e.g. computing PWC at *Spa* using RWC obtained out of *Florennes*). The results of both self- and cross-prediction computations are shown and commented in Section 3.1.
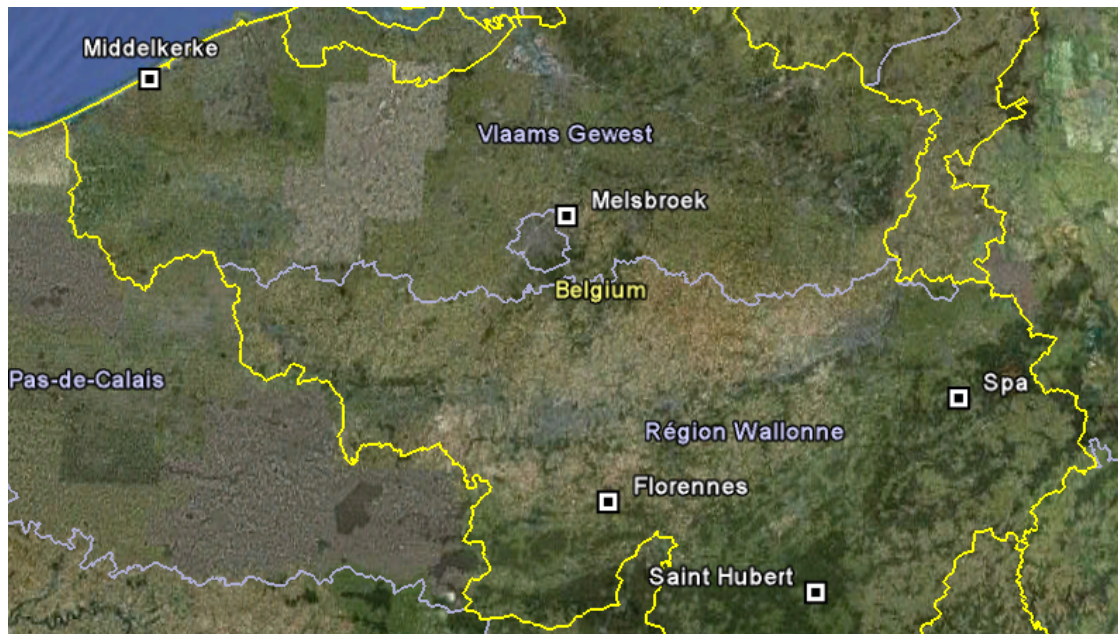
Figure 2.9: Northern Europe meteorological stations in the European Wind Atlas used in the context of this study.

Figure 2.10: Southern Europe meteorological stations in the European Wind Atlas used in the context of this study.

2.3.2 Setup

The following paragraphs describe briefly the setup of the most relevant variables necessary to compute PWC using *WAsP* and how those data can be obtained:

Terrain elevation In order to model topographic effects, *WAsP* needs to be provided with terrain-elevation data. Data of surface height can be freely obtained out of *GTOPO30 global dataset*, a global digital elevation model (DEM) in geographic coordinates (datum WGS84) with a horizontal grid spacing of $30''$ and a vertical resolution of $1m$, which is provided by the United States Geological Survey (USGS, [16]). The conversion from raster format (pixel) to vector–lines (contour lines) is performed by means of Geographical Information System tools (GIS). The results, overlapping both formats, raster and vector, can be observed in Figure 2.11 and 2.12.
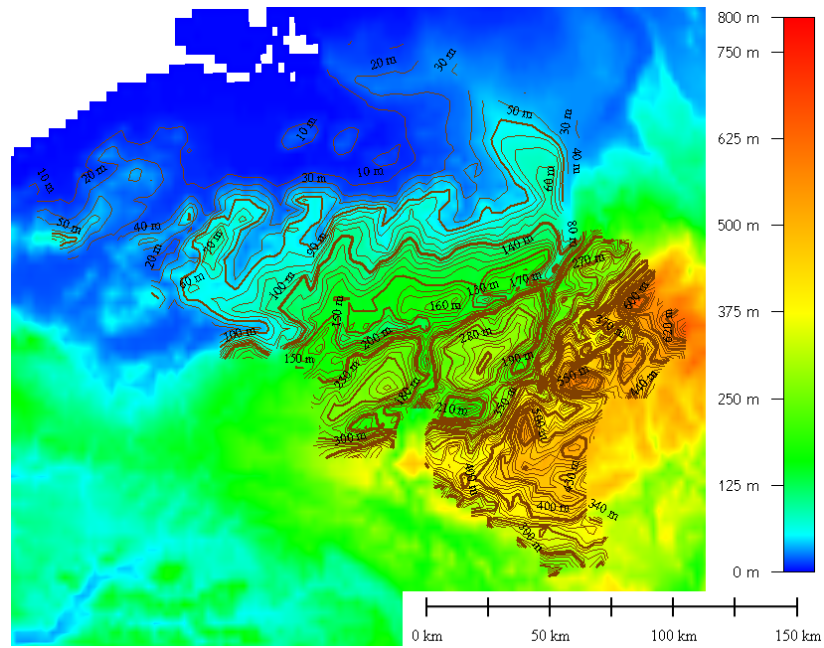
Figure 2.11: Digital elevation model –DEM– and contour lines conversion of the Northern area under study and surroundings (see [16]).
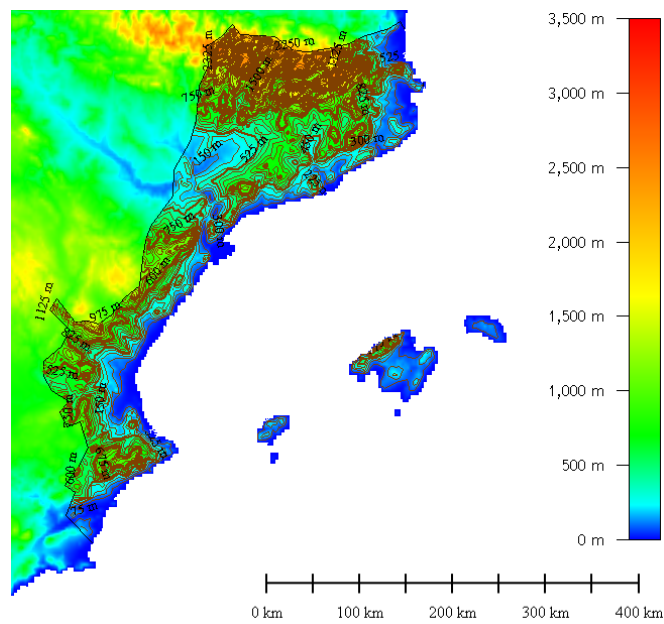
Figure 2.12: Digital elevation model –DEM– and contour lines conversion of the Southern area under study and surroundings (see [16]).

Obstacles shelter Obstacles in the close vicinity of the points under study must be defined according to their dimensions and position. Nevertheless, as no information about them seems to be easy to obtain, a simplification has to be carried out: the closest obstacles to the points under stydy are modeled as roughness, just as farther ones.

Terrain roughness Terrain roughness lenght is obtained out of the *CORINE Land Cover 2000* maps provided by the European Environment Agency (EEA, [17]), with an approximated horizontal resolution of $3''$. Again, in order to adapt the roughness maps (raster) to *WAsP* format (vector–polygon), GIS software has to be used. In this case, the software used is *ESRI ArcGIS 9.3*, *Globalmapper v12* and *WAsP Map Editor*. *WAsP Map Editor*, the tool that handles and converts maps to *WAsP* format cannot deal with polygons defined by more than 32,000 points, threshold easily reached by the *CORINE Land Cover* maps of extense zones. For this reason, all roughness maps have to be cropped to a radius of $20km$ around the point under study[5] and their polygons' vertices smoothened.
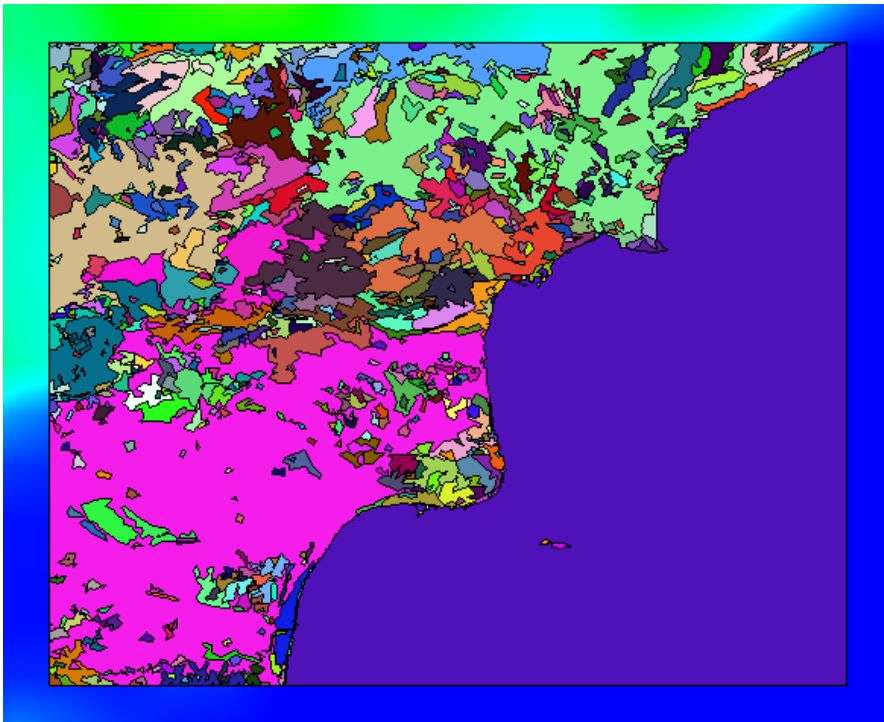
Figure 2.13: Roughness map example (*Alacant*) overlapping digital elevation model.

---

[5]According to [6], in the most unfavorable cases (large roughness length changes), roughness can exert influence on a point at a fetch distance up to $20km$. Out of this radius around the point under study, roughness effects are not taken into account by *WAsP*
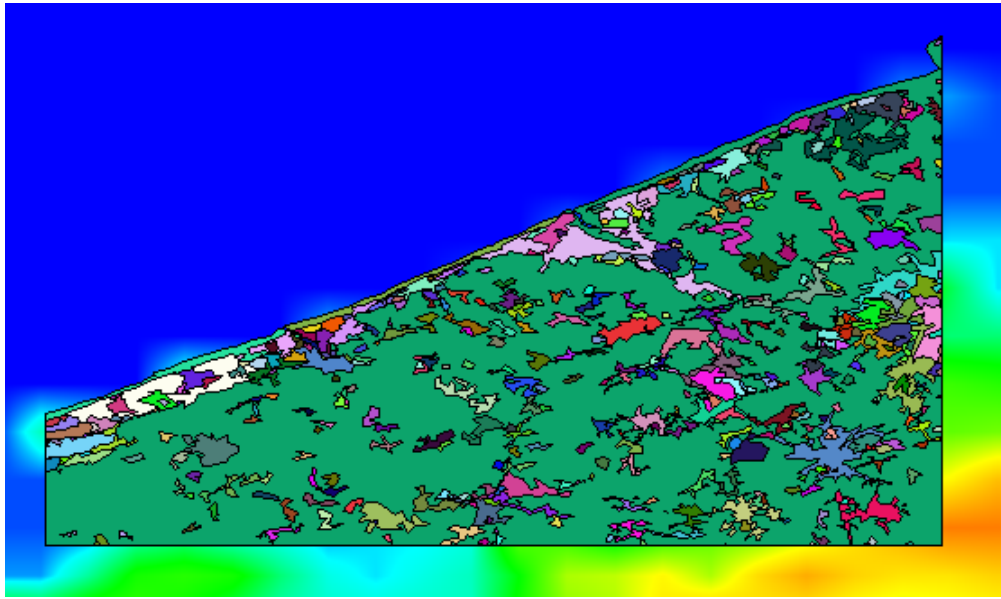
Figure 2.14: Roughness map example (*Middelkerke*) overlapping digital elevation model.

Both elevation and roughness lenght have to be merged into a single map-file in order to be processable by *WAsP*. This can be done by means of *WAsP Map Editor*, one of *WAsP* tools.

Regional wind climate As previously mentioned, wind data for five different stations (regional wind climate or RWC) are used. Such meteorological stations are those mentioned in the beginning of this section (Pag. 23), which are provided by the European Wind Atlas ([7]).

2.4   Downscaling tool

2.4.1   Description

As previously stated, the final goal of the described downscaling tool is to obtain a set of time-marching sector-wise wind velocity profiles out of *NCEP/NCAR Reanalysis Data 1* files (mesoscale model output data) using *WAsP* to refine them. Thus, *WAsP* provides high-resolution sector-wise averaged (static) wind velocity profiles whereas the *NCEP/NCAR Reanalysis Data 1* introduce the time variability of wind velocity and direction. Fig. 2.15 outlines the whole downscaling process and how *NCEP/NCAR Reanalysis Data 1* and *WAsP* data contribute.
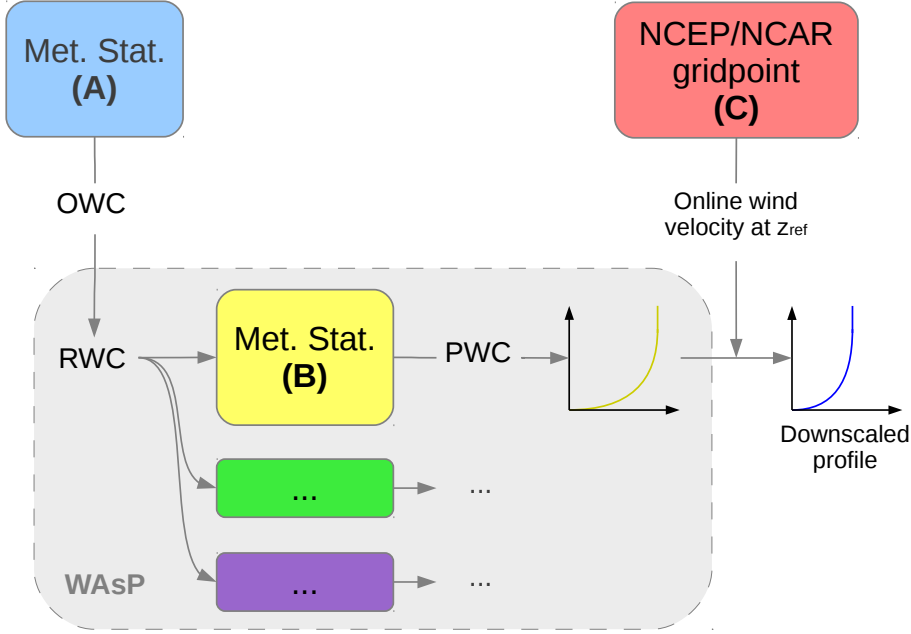
Figure 2.15: Downscaling general scheme: a regional wind climate is obtained out of the observed wind climate at *Point A*. This RWC is used to obtain long-term averaged wind velocities profiles at a *Point B* (i.e. predicted wind climate or PWC). At last, by means of the wind velocity at *Point C* provided by the *NCEP/NCAR Reanalysis Data 1*, time-marching downscaled profiles are obtained at *Point B*.

The link between the wind velocity profiles provided by *WAsP* and the *NCEP/N-CAR Reanalysis Data 1* is made assuming that at a given time, at a given point of the terrain and at a given height (z_{ref}) the wind condition is the same in both the refined and non-refined datasets (i.e. *WAsP* and *NCEP/NCAR Reanalysis Data 1*) and so they are reciprocally convertible, as site-surrounding features do not affect the wind condition. That reference height has to be right between the vertical meso- and microscale in order to be a reliable liaison between them. How it is estimated is discussed in detail in Sec. 2.4.4.

Eq. 2.10 summarizes in an elegant way how both models, *WAsP* and *NCEP/NCAR Reanalysis Data 1*, are correlated. Indeed, this simple equation is the core of the entire downscaling process:

$$u_k(t_j, z_i) = \frac{u_{W,k}(z_i)}{u_{W,k}(z_{ref})} u_{N,k}(t_j, z_{ref}) \tag{2.10}$$

where:

- $u_k(t_j, z_i)$ is the resulting refined wind velocity profile for sector[6] k at time step t_j,

- $u_{W,k}(z_i)$ is the average wind velocity profile provided by *WAsP* for sector k,

- $u_{W,k}(z_{ref})$ is the average wind velocity provided by *WAsP* for sector k at z_{ref},

- $u_{N,k}(t_j, z_{ref})$ is the wind velocity provided by *NCEP/NCAR Reanalysis Data 1* at sector k, at a height of z_{ref} and time t_j.
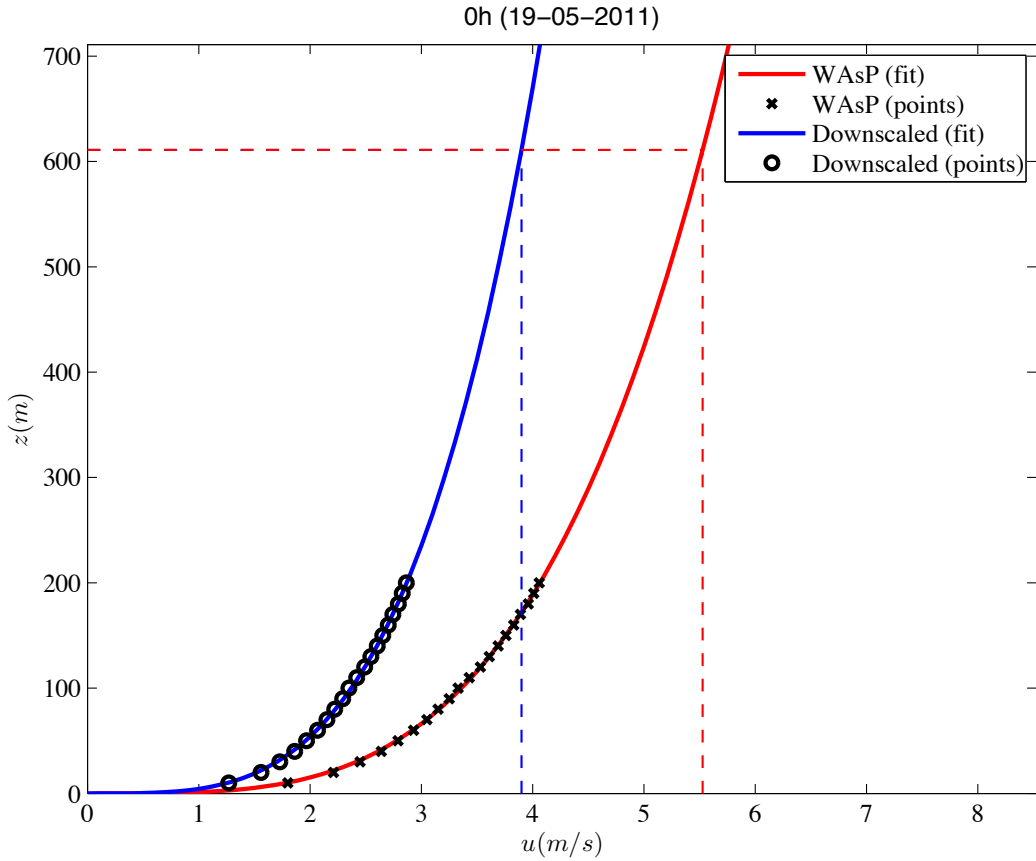
Figure 2.16: Example of wind velocity profiles at a point in Belgium obtained from *WAsP* (wind climate) and the resulting downscaled (time-marching) profile after applying the conversion discussed in Sec. 2.4.1. The dashed line indicates de reference height (z_{ref}), at which the conversion is performed.

---

[6]Sectors to wind direction correspondence may be found in Sec. 2.2.1

Another way to see it is the following: the first term of Eq. 2.10 provides a long-term averaged wind velocity profile, which is adimensionalized with respect to the velocity at the reference height (u_{ref}). Thus, the second term can be seen as a factor representing the wind magnitude and direction with respect to time, which multiplied by the dimension-less profile yields the downscaled wind velocity profile at a given time step (Fig. 2.16 shows the resulting profile $u_k(t_j, z_i)$ –in circles–). It is worth pointing out that, when dealing with *NCEP/NCAR Reanalysis Data 1*, a problem arises: wind profiles are referred to pressure levels instead of geometric height (as in *WAsP*). To overcome this problem, a conversion has to be carried out (all details are explained in Sec. 2.4.2).

This operation and the wealth of secondary operations which have to be performed, from extracting data from their respective files, to comparing the downscaled results against observed wind data, are explained in the following sections and are executed by a single *MatLab* script, which is entirely reproduced in Appx. B.

2.4.2 NCEP/NCAR Reanalysis

This section summarizes step by step the operations performed by the downscaling routine concerning the *NCEP/NCAR Reanalysis Data 1*, from the data extraction to the final obtention of results, which are subsequently downscaled.

Data extraction

The way *NCEP/NCAR Reanalysis Data 1* are processed is the following: such data are downloaded from [18] as *NetCDF*-format files (extension `.nc`) and are extracted by *NCDUMP*, a software freely available online. This program is called by a script executed in *Linux* command line, which is in turn automatically called by *MatLab* when running the downscaling application. The following step consists on correcting the magnitudes of the profile (wind velocity or geopotential height) with the scale factor and the offset using the following expression:

$$x_{act} = x_N \cdot \epsilon - \gamma \tag{2.11}$$

where x_{act} is the actual value, x_N is the non-corrected value provided by the *NCEP/NCAR Reanalysis Data 1*, ϵ is the scale factor and γ the offset, both provided by the *NCEP/NCAR Reanalysis Data 1* files (further information on data format can be found in Appx. A).

Time conversion

Once the data containing horizontal velocities and geopotential height are extracted at their respective directories according to their time step and their format is checked, wind velocity profiles are obtained from such data. The first step consists on converting the time step format from *NCEP/NCAR Reanalysis Data 1* format (hours passed since 0AM, January 1st 1948) to an interpretable one. This is done thanks to a series of *MatLab* libraries[7], which convert seconds passed since 0AM, January 1st 1978 to date and time (it is worth remarking this as no data before this date are accepted by the downscaling routine).

Vertical coordinate conversion

The next step is transforming the vertical coordinate of the profiles provided by the *NCEP/NCAR Reanalysis Data 1* as this data set provides information on several variables (e.g. wind velocity, temperature, etc.) at different heights, but they are expressed as pressure levels instead of as geometric height.

In order to use *NCEP/NCAR Reanalysis Data 1* in combination with *WAsP*, a conversion from pressure levels to geometric height has to be performed. There are several ways to do it (e.g. hydrostatic equation, barometric formula, etc.) but they are normally based on the assumption of constant temperature or constant vertical termperature gradient. Such assumption is only valid in certain stable regimes, but cannot be done systematically.

Hence, another approach is necessary. Although *NCEP/NCAR Reanalysis Data 1* provides temperature values (which makes possible an accurate hydrostatic approach), there is a simpler and more elegant way to convert wind velocity data with respect to pressure levels to geometric-height profiles: via the geopotential height.

The geopotential height is a "gravity-adjusted height" which is widely used in numerical weather prediction (NWP) as it allows neglecting centrifugal forces and air density effects, which are complex to model. Indeed, the geopotential height difference between two consecutive pressure levels is proportional to the mean temperature in that range and such relation is used to perform the afore-mentioned conversion.

The geopotential height is defined as follows:

$$z_g = \frac{\Phi}{g_0} \tag{2.12}$$

---

[7]Libraries available at `http://home.online.no/~pjacklam/matlab/software/util/timeutil/`

being g_0 the gravity acceleration at the sea level in function of latitude (ϕ), which can be estimated in a highly accurate way by means of the *World Geodetic System* (WGS84) expression:

$$g_0 = 9.780327 \frac{1 + 0.00193185 sin^2\phi}{\sqrt{1 - 0.00669438 sin^2\phi}} \tag{2.13}$$

and where Φ is the geopotential, defined as follows:

$$\Phi = \int_0^H g(\phi, z)\, \mathrm{d}z \tag{2.14}$$

being $g(\phi, z)$ the gravity acceleration in function of latitude (ϕ) and height (z), which can be computed as follows:

$$g(\phi, z) = g_0 \left(\frac{r}{r + H} \right)^2 \tag{2.15}$$

where r is the mean Earth radius, defined under a spheroidal approach in function of the latitude (ϕ) and the Earth Equatorial and Polar Radii (according to the WGS84: $r_e = 6,378,137m$ and $r_p = 6,356,752m$, respectively), as follows:

$$r = \sqrt{\frac{(a^2 \cdot cos(\phi))^2 + (b^2 \cdot sin(\phi))^2}{(a \cdot cos(\phi))^2 + (b \cdot sin(\phi))^2}} \tag{2.16}$$

and H is the the total geometric height above the sea level, i.e. the sum of the terrain elevation above the sea level and the height above the ground level ($h_{terr} + z$).

Bearing this in mind, out of [21] it can be demonstrated that the relation between geopotential and geometric height is the following:

$$H = \frac{z_g Q}{r + z_g} \tag{2.17}$$

being $Q = r \frac{g_0}{9.80665 \frac{m}{s^2}}$ the gravity ratio.

Since *NCEP/NCAR Reanalysis Data 1* provides both wind velocity and geopotential height at the same given point, pressure level and time, thanks to Eq. 2.17, wind velocities can be easily expressed as a function of geometric height.

Wind velocity and direction profiles

The last operation concerning *NCEP/NCAR Reanalysis Data 1* is computing the modulus of the wind velocity vector and its direction. They are computed respectively by the following well-known trigonometric identities:

$$u_N = \sqrt{U^2 + V^2} \tag{2.18}$$

$$\beta = arctan \left(\frac{V}{U} \right) \tag{2.19}$$

Obviously, directions have to be represented in sectors in coherence with *WAsP* data (otherwise, they would not be compatible). Once all those actions have been performed, the *NCEP/NCAR Reanalysis Data 1* profiles for every time step can be plotted and saved in a text file. Fig. 2.17 shows an example of the resulting wind velocity profile obtained out of *NCEP/NCAR Reanalysis Data 1* at a given time step.

The horizontal dashed line at the bottom of the plot is the highest point of the profile provided by *WAsP* by default. Here one can observe the large difference of scales between *WAsP* and the *NCEP/NCAR Reanalysis Data 1* (even the lowest point of the mesoscale-model data is above the microscale-model default limit).

Indeed, unlike *WAsP*, the *NCEP/NCAR Reanalysis Data 1* cannot be approached to a logarithmic profile. Instead, more complex profiles occur, even several mesoscale phenomena may eventually arise, such as Ekhman layers in convective cells. In the example shown (see Fig. 2.17), one can perfectly see the boundary between the troposphere and the stratosphere (i.e. tropopause) delimited by a sudden change of sign of the air temperature gradient. At this layer, no vertical flow occurs but jet streams may appear instead, as in the case shown (wind-velocity peak at $1200m$).
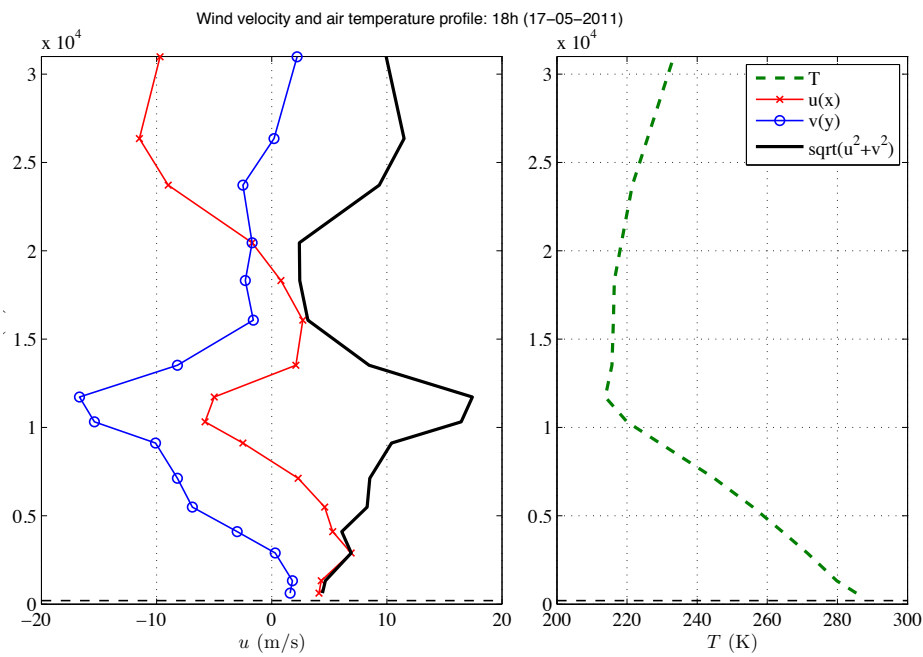
Figure 2.17: Example of *NCEP/NCAR Reanalysis Data 1* profiles of wind velocity (vector components and resulting modulus) and air temperature. Positive directions in the x- and y-axes are East to West and South to North, respectively. The dashed line in the bottom of the plot denotes the upper limit of *WAsP* model scale, which shows the large scale difference between both models used.
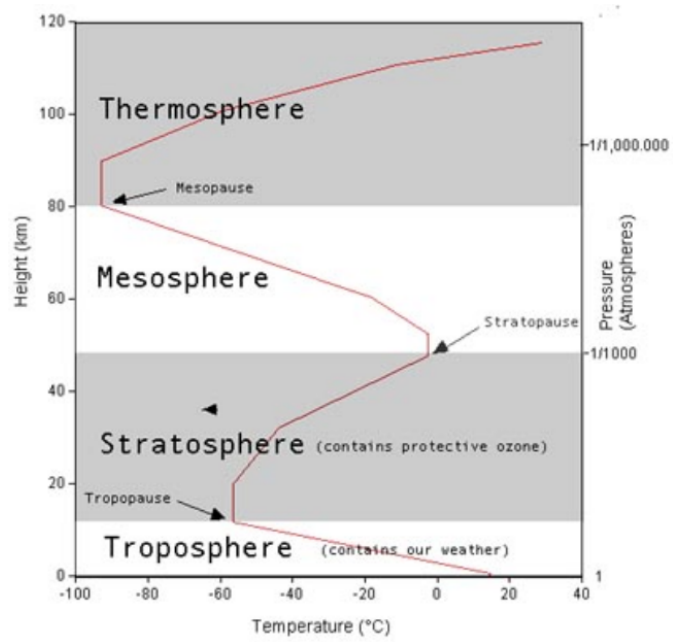
Figure 2.18: Layers of the Earth Atmosphere according to its temperature gradients.

2.4.3 WAsP

As regards *WAsP* data, only the predicted wind climate (PWC) files at heights from $10m$ to $200m$ (at $10m$-intervals) have to be introduced to the downscaling tool (see Appx. A). Those data can be obtained in the menu *Turbine Site Report* of the *WAsP* GUI. The PWC must be computed at the point under study out of RWC obtained at any point which can be considered within the same region in terms of overall wind climate, to fulfill *WAsP* most important assumption (see Sec. 2.2.1).

First of all, the file formats are checked and some inconvenient characters are removed by means of a simple script executed at the *Linux* command line, which is automatically called by *MatLab*. The next step consists on extracting the sectorwise Weibull parameters (A and q) at every height from $10m$ to $200m$ out of the PWC files. Using those values, by means of Eq. 2.1, the velocities at every height and at every sector are computed, resulting a set of 12 mean velocity profiles, one for each sector.

At last, the points of the profiles obtained are respectively fitted to potential curves in order to inter- and extrapolate other points. Once these actions have been performed, the afore-mentioned wind velocity profiles can be plotted and saved to text files. Fig. 2.19 shows an example of the resulting wind velocity profile at a given sector.
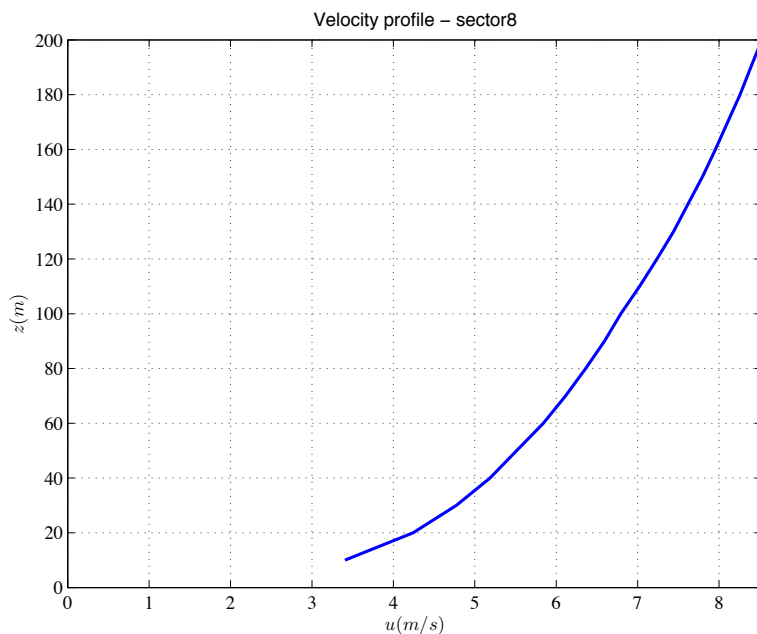
Figure 2.19: Example of *WAsP* profile: the points of the profile are given by the wind-speed mean Weibull-distribution values (see Sec. 2.2.1 on Pag. 14) given by *WAsP* at every height.
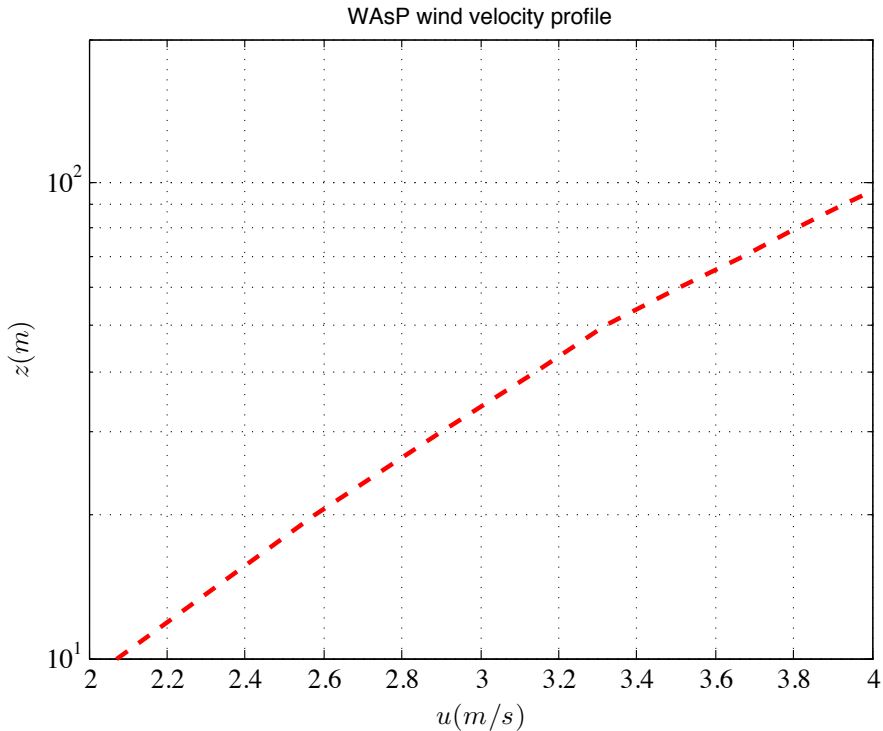
Figure 2.20: Example of *WAsP* logarithmic profile (the fractures in the line denote irregularities in the profile, which are produced by the development of IBLs).

2.4.4 Reference height

At this point, it is necessary to determine the reference height (z_{ref}) at which both data, *WAsP* output and the *NCEP/NCAR Reanalysis Data 1*, can be correlated. Recalling Eq. 2.7, under the most unfavorable conditions, the maximum height at which site effects are felt in *WAsP* is approximately $h'(max) = 1440m$. Furthermore, according to [7], in coastal regions, wind conditions at a pressure level of $850mb$ (approximately, a height of $1500m$) can be considered representative of the geostrophic wind conditions.

One may think that this should be the reference height at which information can be exchanged between both models. Nevertheless, bearing in mind that *WAsP* profile highest point is by default $200m$, at $1500m$ such profiles may be no longer representative of near-surface conditions. In addition, the geostrophic wind condition is the "site-effect free" wind condition (see discussion on Sec. 2.2.1 on Pag. 15) and therefore it cannot be compared to *WAsP* predicted wind climates (site-effect affected)[8].

---

[8]Although the chosen approach to determine z_{ref} is the lowest *NCEP/NCAR Reanalysis Data 1* point, taking $z_{ref} = 1500m$ is also tried thanks to a little modification of the downscaling application (see Appx. B). The results are commented in Sec. 3.2.

For this reason, as lower points ($1000mb$ and $925mb$) are often available in the *NCEP/NCAR Reanalysis Data 1*, the criterion to establish a reference height (at which wind velocities are assumed to be reciprocally convertible, i.e. z_{ref}) is the *NCEP/NCAR Reanalysis Data 1* lowest available point since, although such point may be out of the *WAsP* vertical scale, it is generally still close.

It is important pointing out that, as such profiles are provided with respect to pressure levels instead of geometric heights, vertical coordinates are not constant from one time step or location to another. Indeed, the lowest pressure level ($1000mB$) may happen to be below the terrain level in many cases (especially, at mountainous regions, where surface pressure is always lower than $1000mB$). Therefore, the reference height is the lowest *NCEP/NCAR Reanalysis Data 1* point among those which, after converting from pressure level to geometric coordinates, happens to be above the terrain level.

2.4.5 Downscaling

Once *WAsP* data and the *NCEP/NCAR Reanalysis Data 1* have been properly processed, in order to perform the downscaling process itself, first of all, all the involved data (*NCEP/NCAR Reanalysis Data 1* and *WAsP*) have to be loaded. At this point, Eq. 2.10 can be applied. The points of the resulting profile ($u_k(t_j, z_i)$) are the final results of the downscaling tool.

Such profiles, as it is done to *WAsP*-profile points, are fitted to a potential curve in order to compute velocities at points different from those at which profiles are defined and saved in a text file for the subsequent validation process. Fig. 2.15 on Pag. 29 summarizes the whole downscaling process.

2.4.6 Validation

The validation of results yield by the downscaling tool is automatically performed by the *MatLab* routine as long as meteorological station observations are provided. This is done comparing downscaled values (following the downscaling process discussed above) to field observations (meteorological-station measurements). The default period of comparison is $48h$ (8 time steps, as $\Delta t = 6h$) and data of wind speed and direction (sector) must be introduced in a text file in the *./observations* directory.

After loading the downscaled data and the meteorological station observations, the height of the meteorological station mast has to be provided by the user. Thanks to the latter value and the potential fit mentioned in Sec. 2.4.6, the wind velocity provided by the downscaling tool can be computed at every time step and compared to the appropriate observed value.

In order to assess the accuracy of the results yielded by the developed downscaling tool, two episodes are tested at two different locations: the period between 17th and 19th of Mars 2011 in *Wideûmont* (Belgium) and the period between 22th and 24th of July 2011 in *Carcaixent* (València). The necessary field observations are provided by the *Institut Royal Meteorologique (IRM)*[9] and the *Agencia Estatal de Meteorología (AEMET)*[10], respectively.

What is done in this part of the project is applying the methodology explained to two test cases, in which wind velocity is to be predicted at two meteorological stations and compared to their measurements. Recalling the nomeclature in the general scheme of the downscaling tool (see Fig. 2.15 on Pag. 29), in each tested case the points are the following:

Test case 1

– Point A: *Saint-Hubert (Belgium)*.
– Point B: *Wideûmont (Belgium)*.
– Point C: *Lat.: 50N – Long.: 5E*.

Test case 2

– Point A: *Carcaixent (València)*.
– Point B: *Carcaixent (València)*.
– Point C: *Lat.: 40N – Long.: 0*.

The distance between points in case no. 1 ranges from $15km$ to $30km$ (see Fig. 2.21), whereas in case no. 2, points are separated by distances up to more than $100km$ (see Fig. 2.22). The main advantage of the latter is that the station from which the regional wind climate (RWC) is obtained (Point A) and that where the validation data is harvested (Point B) match.

---

[9]Data available at: `http://www.meteo.be/meteo/view/fr/123386-Observations+-+meteo.html`
[10]Data available at: `ftp://ftpdatos.aemet.es/datos_observacion/`
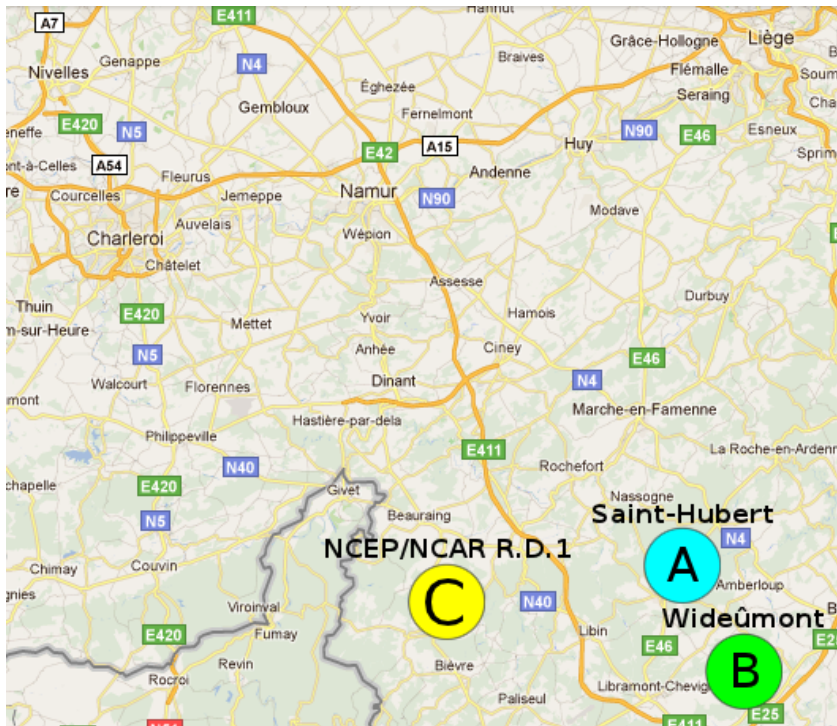
Figure 2.21: Map of points of the case under study no. 1: *Point A: Saint-Hubert (Belgium), Point B: Wideûmont (Belgium), Point C: NCEP/NCAR Reanalysis Data 1 grid point of geographic coordinates 50N-5E.*
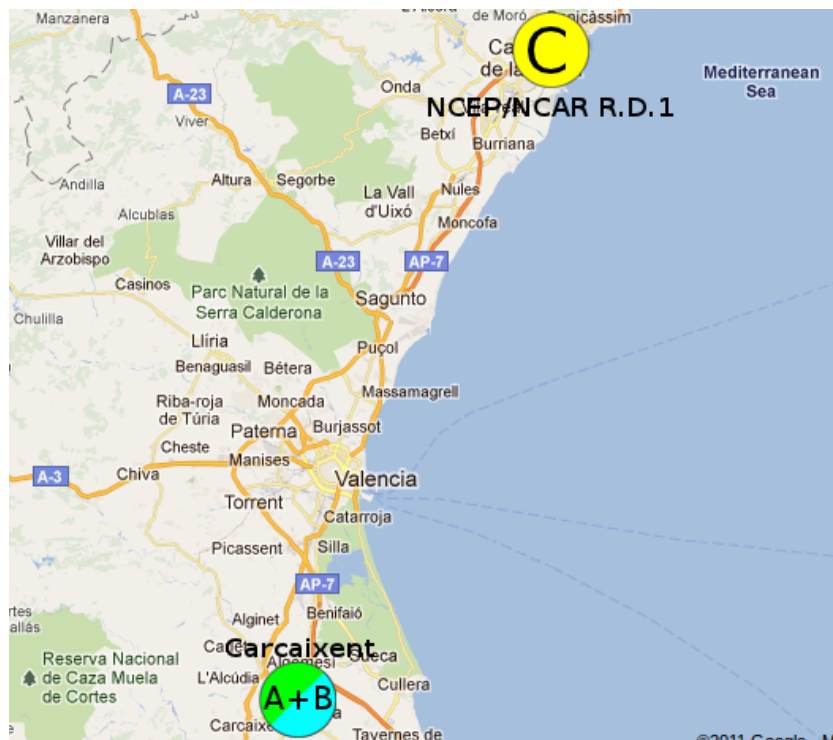
Figure 2.22: Map of points of the case under study no. 2: *Point A: Carcaixent (València), Point B: Carcaixent (València), Point C: NCEP/NCAR Reanalysis Data 1 grid point of geographic coordinates 40N-0.*

Chapter 3

Analysis of results

This section reproduces and comments the results obtained regarding the two main lines of this project: the obtention of a wind atlas of two zones of Europe (as explained in Sec. 2.3), including their comparison to the wind atlas of the same points computed previously by other authors, and the development and subsequent validation of a downscaling tool which uses *WAsP* to refine *NCEP/NCAR Reanalysis Data 1* (as explained in Sec. 2.4).

3.1   Wind map

3.1.1   Self- and cross-prediction

Tab. 3.1 and 3.2 show the self- and cross-prediction results of the computed wind atlas, i.e. predictions performed at the same points where meteorological data were obtained and performed at a different points, respectively (see Fig. 2.4). To measure the accuracy of every station's measurements, the values in each row (cross-predictions) have to be compared to the correspondent diagonal value (self-predictions, in bold). This way of assessing accuracy hinges on the assumption, according to [6], that relative errors of less than 2% are expectable in *WAsP* for self-predictions, provided a good description of the terrain. For this reason, they can be used as a reference value to compare cross-predictions.

In prediction of wind resources for sites different from the measured (i.e. cross-prediction), good agreement with actual values can be generally reached, except for meteorological stations at or near the coast, "where the impact of the sea wind climate can be easily explained in terms of other stability regimes when the fetch over sea is long enough" ([3]).

Table 3.1: Results obtained by the author: self- and cross-prediction comparison of mean wind speed at $10m$ a.g.l. at the five meteorological stations studied in Northern Europe (Mdk: *Middelkerke*, Mls: *Melsbroek*, Spa: *Spa*, Sth: *Saint-Hubert*, Flr: *Florennes*). Columns show the station from which the regional wind climate is computed and rows that on which is computed (diagonal terms correspond to self-prediction).

$\frac{m}{s}$	Mls	Flr	Sth	Spa	Mdk
Mls	**4.2**	4.2	4.1	4.4	4.8
Flr	2.6	**2.5**	2.6	2.6	3.1
Sth	4.7	4.5	**4.4**	4.6	5.1
Spa	4.0	3.8	3.8	**3.9**	4.3
Mdk	4.3	4.1	4.2	4.5	**4.7**

Table 3.2: Results obtained by the author: self- and cross-prediction comparison of mean wind speed at $10m$ a.g.l. at the five meteorological stations studied in Southern Europe (Ala: *Alacant*, Bcn: *Barcelona*, Gir: *Girona*, Mal: *Mallorca*, Men: *Menorca*, Vlc: *València*). Columns show the station from which the regional wind climate is computed and rows that on which is computed (diagonal terms correspond to self-prediction).

$\frac{m}{s}$	Ala	Bcn	Gir	Mal	Men	Vlc
Ala	**3.9**	3.1	2.4	2.7	4.5	3.2
Bcn	3.6	**2.9**	2.2	2.7	4.1	2.9
Gir	3.8	3.0	**2.2**	2.8	4.1	3.0
Mal	2.6	2.1	1.7	**1.7**	2.9	2.0
Men	3.2	2.4	1.7	2.4	**3.8**	3.0
Vlc	4.4	3.9	2.7	3.2	5.1	**3.5**

As regards Tab. 3.1, it is remarkable that, despite the large domain considered, whose order of magnitude is out of the WAsP computational envolope (microscale), the model is fairly accurate (relative errors below 7% extrapolating wind climate to points farther than $100km$ away), except for the *Middelkerke* case. The reason for this unusual high accuracy is the high uniformity of the Belgian inland meteorological conditions, due essentially to its smooth orography.

Nevertheless, as mentioned above, not all the cases' performance is that good: *Middelkerke* station fails to reproduce other stations wind climate condition and, in turn, the other stations cannot predict properly *Middelkerke* wind climate either (relative errors around 25% extrapolating at distances below $100km$ occur). This is due to the fact that the afore-mentioned station is at about only $1km$ away from the coastline, with no obstacles in the middle (see Figure 3.1). Therefore, its wind climate is highly influenced by the off-shore meteorological conditions. Fig. 3.2 and 3.3 show a wind-rose and non-directional wind-speed distribution comparison in which one can see the wind climate difference between both sites.
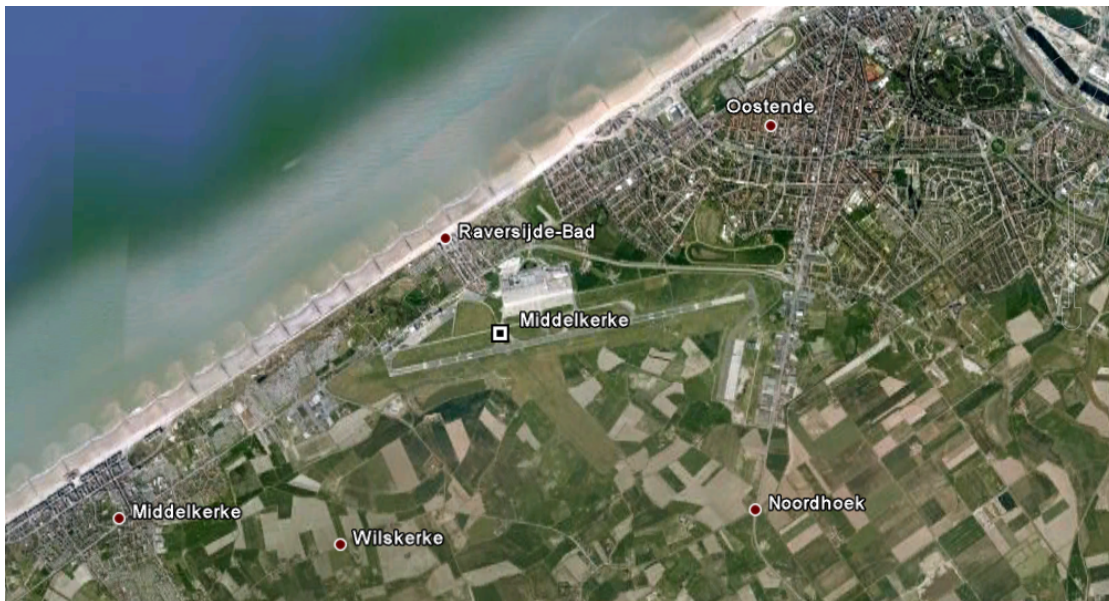
Figure 3.1: *Middelkerke* meteorological station.

Large efforts are currently done by the wind-energy industry and research community in order to achieve good accuracy in wind condition forecasting in coastal and off-shore areas, as wind farms in such places are becoming more and more frequent, but there is no consensus yet. Obviously, due to their high cost, before off-shore wind farms are built, an accurate beforehand wind-resource assessment is necessary.
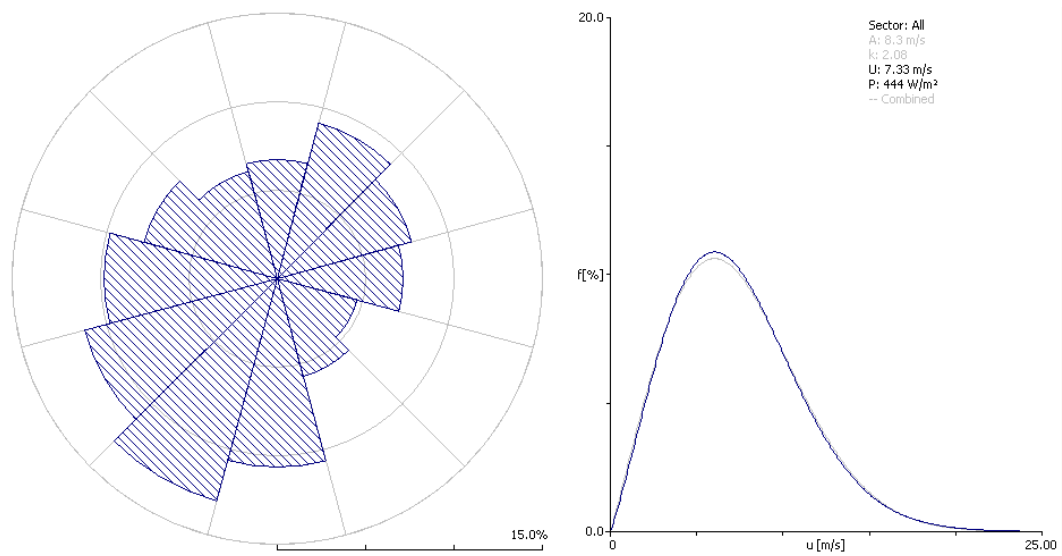
Figure 3.2: *Middelkerke* regional wind climate wind rose and Weibull distribution.
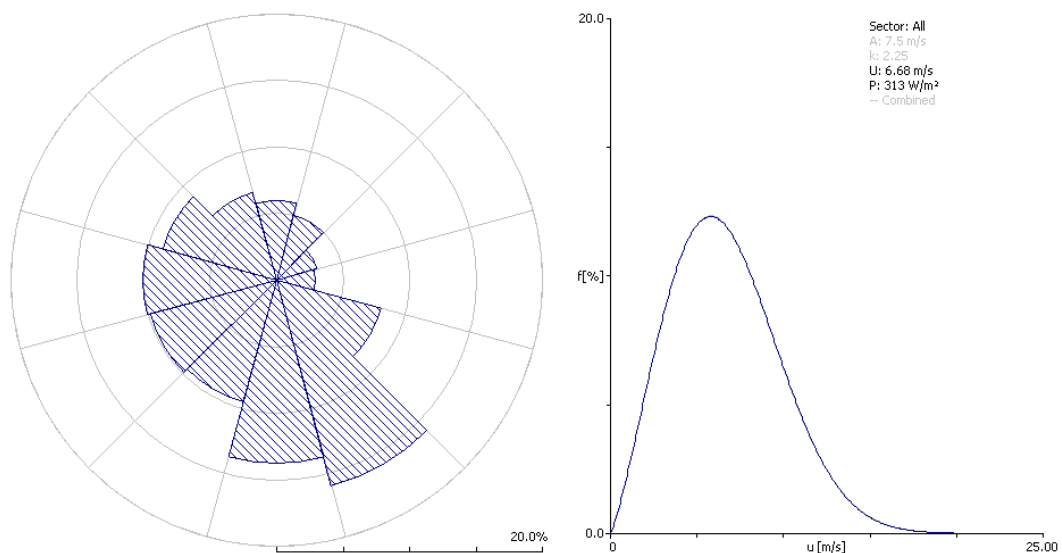
Figure 3.3: *Spa* regional wind climate wind rose and Weibull distribution.

As regards Tab. 3.2, errors are much larger, but so are distances. Relative errors above 80% between non-coastal continental stations and those placed on islands occur (e.g. from *Menorca* to *Girona*). Between two continental stations errors above 65% are found (e.g. from *Alacant* to *Girona*). Nevertheless, these stations are affected by coastal and inland climatic conditions, respectively, and are more than $500km$ away, which exceeds more than 10 times *WAsP*'s computational domain. All Southern Europe stations studied are too far from each other to expect coherent cross-prediction results.

3.1.2   Previous experiments

This very same experiment but with no roughness simplification is carried out by [7] before 1989 (see Tab. 3.3 and 3.4), obtaining similar results regarding Northern Europe to those exposed in Tab. 3.1: good predictions for all of the stations, except for *Middelkerke* (both when being used to predict and when being predicted).

Table 3.3: Results obtained by [7]: self- and cross-prediction comparison of mean wind speed at $10m$ a.g.l. at the five meteorological stations studied in Northern Europe (Mdk: *Middelkerke*, Mls: *Melsbroek*, Spa: *Spa*, Sth: *Saint-Hubert*, Flr: *Florennes*). Columns show the station from which the regional wind climate is computed and rows that on which is computed (diagonal terms correspond to self-prediction).

$(\frac{m}{s})$	**Mls**	**Flr**	**Sth**	**Spa**	**Mdk**
Mls	**4.4**	4.3	4.3	4.4	4.9
Flr	4.0	**3.9**	3.9	4.1	4.5
Sth	4.5	4.3	**4.3**	4.4	5.1
Spa	4.1	4.0	4.0	**4.2**	4.6
Mdk	5.2	5.0	5.0	5.2	**5.8**

Table 3.4: Results obtained by [7]: self- and cross-prediction comparison of mean wind speed at $10m$ a.g.l. at two of the meteorological stations studied in Southern Europe (Ala: *Alacant*, Vlc: *València*). Columns show the station from which the regional wind climate is computed and rows that on which is computed (diagonal terms correspond to self-prediction).

$\frac{m}{s}$	*Vlc*	*Ala*
Vlc	**3.3**	4.0
Ala	3.2	**3.9**

Despite the fact that, as mentioned in the previous paragraph, the same trends are found in both computed wind atlases, there is an important difference between both results: mean wind speeds obtained by [7] are in average more than 10% higher than those obtained in this project.

According to [19], average wind speeds in Belgium decreased approximately 10% since the 1980s due to global-scale meteorological phenomena and land-use change, as one can observe in Fig. 3.4. This is likely the most important reason why the results obtained by [7] are sensitively higher (11.2%) than those obtained in the context of this thesis, although a simplified description of the obstacles or different criteria when estimating roughness lengths around the points under study may also be a reason.
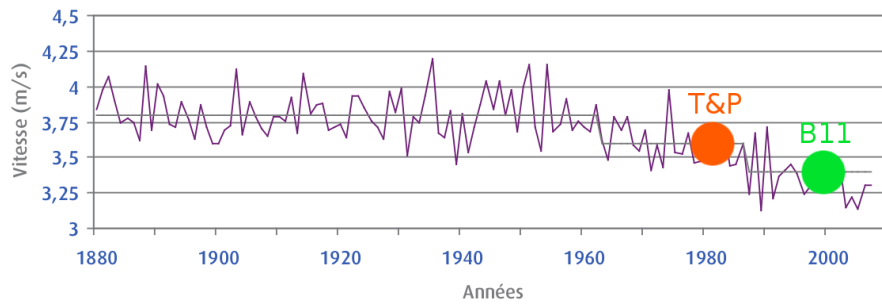
Figure 3.4: Mid-term mean wind velocity evolution in *Brussels* ([19]). The dots correspond to the time at which data for experiments by [7] and for this project computations where respectively obtained.

As regards Southern Europe, less meteorological stations are compared by [7] (only *València* and *Alacant*, see Tab. 3.4) and the results are good (mean relative errors below 5%), sensitively better than those obtained in the Northern Europe case.

3.2 Downscaling tool

This section presents and comments the results obtained testing the downscaling tool in two 2-day episodes at two different sites in Europe. As explained in Sec. 2.4, the information obtained consists on time-marching profiles of wind velocity and direction, which is presented and discussed in Sec. 3.2.1 and 3.2.2, respectively.

3.2.1 Wind velocity

Tab. 3.5 and 3.6 show the wind velocity evolution computed using the downscaling tool and that observed at the meteorological stations of *Carcaixent* and *Wideûmont*, respectively.

At a first sight, one can see that there is a large mismatch between the values obtained by downscaling meteorological data and the field measurements. Nevertheless, in some cases, at least some trends are followed, which is quite an achievement, as atmospheric flow is highly chaotic and is therefore affected by very large uncertainties. In both cases, a clear daily pattern of recurrence arises. Therefore, the following step is finding out how the offset and scale factor between computed and observed data can be reduced to the lowest possible value (i.e. calibrating the model).

Table 3.5: Wind velocity validation in *Carcaixent* (see Fig. 3.5). Values computed by means of the proposed downscaling tool are compared to those observed at the same point and time step.

Date and time	$u_{computed}(\frac{m}{s})$	$u_{observed}(\frac{m}{s})$
22/07/11 (6h)	6.18	2.86
22/07/11 (12h)	3.54	4.50
22/07/11 (18h)	4.40	3.00
23/07/11 (0h)	2.86	1.01
23/07/11 (6h)	1.17	1.27
23/07/11 (12h)	0.65	3.71
23/07/11 (18h)	1.15	3.27
24/07/11 (0h)	1.72	1.29

Table 3.6: Wind velocity validation in *Wideûmont* (see Fig. 3.6). Values computed by means of the proposed downscaling tool are compared to those observed at the same point and time step.

Date and time	$u_{computed}(\frac{m}{s})$	$u_{observed}(\frac{m}{s})$
17/05/11 (6h)	4.50	8.30
17/05/11 (12h)	3.37	8.10
17/05/11 (18h)	2.54	6.90
18/05/11 (0h)	2.27	2.80
18/05/11 (6h)	3.14	4.90
18/05/11 (12h)	2.02	8.00
18/05/11 (18h)	2.11	7.00
19/05/11 (0h)	1.68	2.80

In the *Wideûmont* case, a systematic underestimate of velocities occurs, which may be caused by several reasons; one of them is an overestimate of the terrain roughness length, but also a poor description of the surrounding obstacles of the meteorological station. Nevertheless, other reasons are likely involved in the still large mismatch between computed and observed values, among which it is worth pointing out the following:

Large scale difference between *WAsP* and the *NCEP/NCAR Reanalysis Data 1*, which can be graphically seen in Fig. 2.17, may be play a paramount role in the lack of accuracy of computations.

Low-quality of data out of which computations are carried out may also be important. E.g.: wind velocity and direction are harvested by hand, in-situ description of the obstacles near to points under study is not carried out, but they are modeled as roughness, etc.

The root mean squared error (RMSE) in the *Carcaixent* case is $2.0\frac{m}{s}$, which is approximately 76% of the observed mean value. In wind energy assessment, there is common agreement in considering an error of 10% the threshold of acceptance of NWP-results. In the case of *Wideûmont*, the RMSE reaches $3.9\frac{m}{s}$ (37% of the mean observed value), being thus all results regarding wind velocity not validated.

As mentioned in Sec. 2.4.4, an approach using $z_{ref} = 1500m$ as reference height is also tried thanks to a little modification of the *MatLab* routines. The results, compared to the lowest-point approach in Fig. 3.5 and 3.6, respectively, not only are not improved, but even the main trends are not followed eventually. For this reason, taking the lowest *NCEP/NCAR Reanalysis Data 1* point as reference height (z_{ref}) is kept as the best approach.
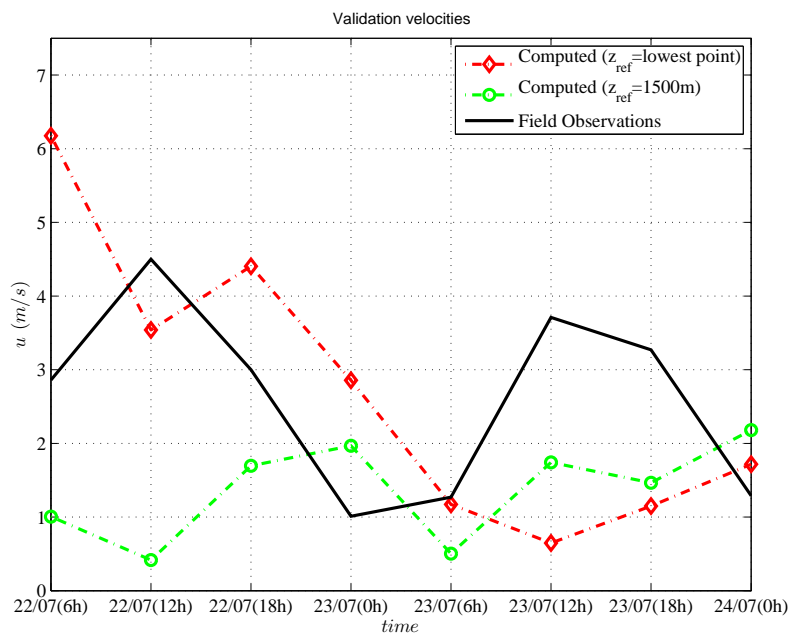
Figure 3.5: Validation of wind velocities computed by the downscaling tool with meteorological observations of *Carcaixent* between the 22th and 24th July 2011.

Figure 3.6: Validation of wind velocities computed by the downscaling tool with meteorological observations of *Wideûmont* between the 17th and 19th May 2011.

3.2.2 Wind direction

As regards wind direction estimate, the results are slightly more encouraging. Tab. 3.8 and 3.9 show respectively the values computed by the downscaling tool and those observed at the meteorological stations of the tested points used to validate the results. Note that directions are represented by sectors, as *WAsP* does. Recalling Sec. 2.2.1 on Pag. 15, the wind rose is split in 12 sectors, spanning each sector 30° and being the sectors clockwise enumerated from 1 to 12 starting in the North.

Table 3.7: Wind direction validation in *Carcaixent* (see Fig. 3.8). Values computed by means of the proposed downscaling tool are compared to those observed at the same point and time step (each sector mismatch is equivalent to 30°).

Date and time	$sector_{computed}$	$sector_{observed}$
22/07/11 (6h)	2	2
22/07/11 (12h)	2	2
22/07/11 (18h)	2	3
23/07/11 (0h)	2	4
23/07/11 (6h)	3	5
23/07/11 (12h)	3	2
23/07/11 (18h)	5	2
24/07/11 (0h)	6	6

Table 3.8: Wind direction validation in *Wideûmont* (see Fig. 3.9). Values computed by means of the proposed downscaling tool are compared to those observed at the same point and time step (each sector mismatch is equivalent to 30°).

Date and time	$sector_{computed}$	$sector_{observed}$
17/05/11 (6h)	4	4
17/05/11 (12h)	4	3
17/05/11 (18h)	3	3
18/05/11 (0h)	4	4
18/05/11 (6h)	3	3
18/05/11 (12h)	3	3
18/05/11 (18h)	3	3
19/05/11 (0h)	4	1

The mismatch is in general very low, especially, if one takes into account that data are treated in a discrete way (in 12 sectors, see Sec. 2.2.1). That means that two points which, apparently, are separated by 30° may be almost overlapping (or separated by almost 60°). One must also take into account, as regards the *Carcaixent* case, that values close to 0° and 360° are actually close to each other.

The RMSE comparing downscaled and observed wind directions is in the *Carcaixent* case 45°, represents the 12% of the complete wind rose (360°). In the *Wideûmont* case, the RMSE is 34° (9%). Bearing in mind that errors up to 30° (one sector) are widely accepted in wind direction predictions, the results obtained during the development of this thesis would not be validated, although they are significatively closer than those regarding wind velocity.

As in the case of the wind velocities, a daily pattern of recurrence arises. It is important pointing out that the wind direction is determined by the *NCEP/NCAR Reanalysis Data 1* (provided at an approximate height of up to 500 or 1000m and different location) and compared to meteorological station observations (measured at a height of 50m or less). Out of this fact, it can be explained the afore-mentioned pattern: as shown in Fig. 3.7, wind directions at different heights tend in general to the same values during the stable conditions of the day, whereas they diverge during the night. Indeed, back to the validation of the downscaling tool results, one can see that the highest differences between observed and computed values (provided at different heights) arise by night.
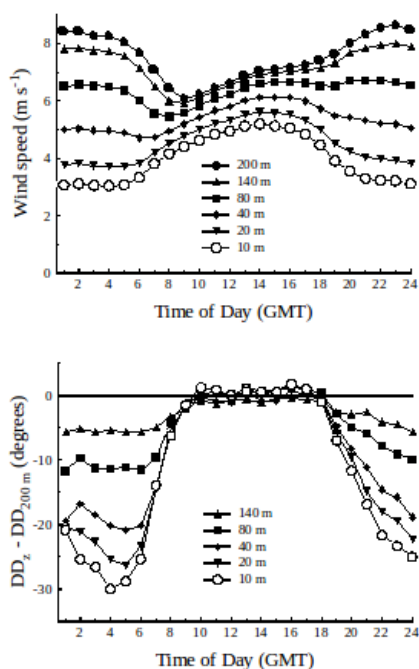
Figure 3.7: Hourly evolution of wind velocity and direction measured in field in *Cabauw (Holland)*, a meteorological mast of more than 200m high.
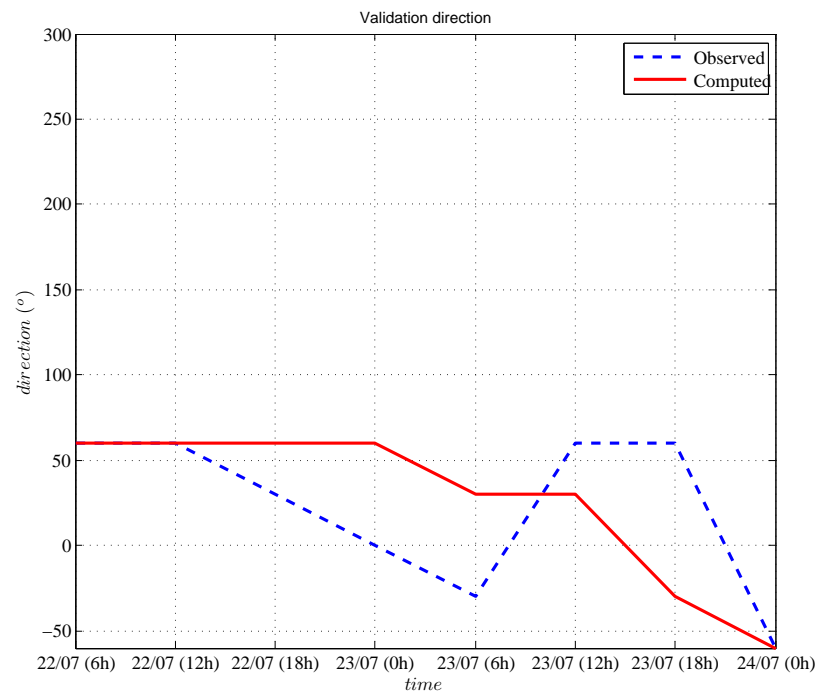
Figure 3.8: Validation of wind directions computed by the downscaling tool with mete-orological observations of *Carcaixent* between the 22th and 24th July 2011.
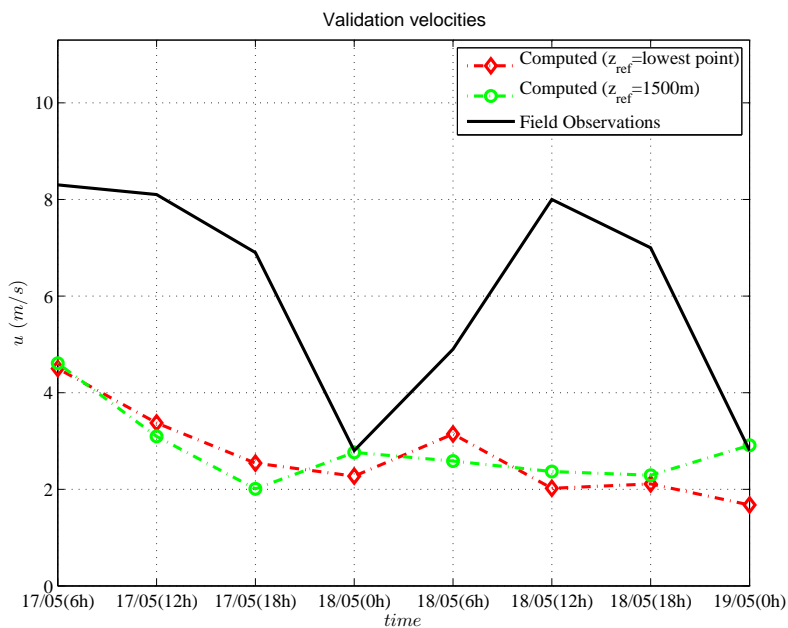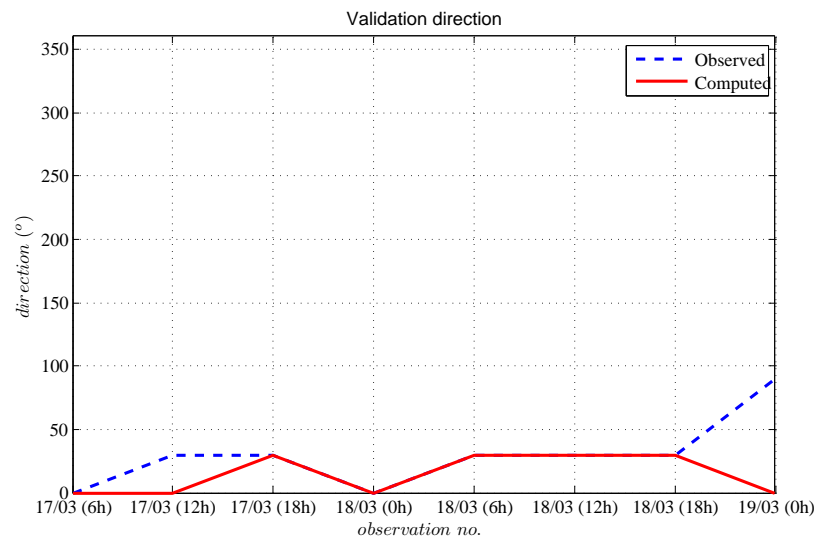

Figure 3.9: Validation of wind directions computed by the downscaling tool with mete-orological observations of *Wideûmont* between the 17th and 19th May 2011.

3.2.3 Richardson number

A last attempt to find the causes of the large mismatch between computed and observed values is done by estimating the Richardson number (Ri), i.e. the ratio between the potential to the kinetic energy of a flow. This dimensionless number of Fluid Mechanics can be computed as follows:

$$Ri = \frac{gh_*}{u^2}$$

where:

- g is the gravity,

- h_* is a representative vertical lengthscale,

- u is the velocity,

Nevertheless, when studying oceanic or atmospheric flows, the Richardson number is commonly expressed replacing the vertical lengthscale by the velocity, pressure and temperature vertical gradients, yielding:

$$Ri = \frac{g}{\theta} \frac{\frac{d\theta}{dz}}{(\frac{du}{dz})^2}$$

where:

- $\theta = T\frac{p}{p_o}$ is the potential temperature,

- p is the pressure,

- p_0 is the pressure on the ground surface[1].

As one can see, on the one hand, the smaller the Richardson number is, the more important buoyancy forces become. On the other hand, the larger it is, the more the flow is driven by its kinetic energy (intertial forces). If the Richardson number is of order unity, then the flow is likely to be buoyancy-driven: although kinetic and potential energies are balanced, the energy of the flow is considered to derive originally almost exclusively from the potential energy.

---

[1] The Richardson number is computed using the values at the two lowest *NCEP/NCAR Reanalysis Data 1* points (i.e. $\frac{d\chi_i}{dz} = \frac{\chi_2 - \chi_1}{z_2 - z_1}$), as points right on the terrain surface are not available. For this reason, the Ri values obtained are not 100% representative of the microscale stability conditions, but for guidance.

In practice and as regards atmospheric-flow studies, the Richardson number is widely used in NWP as it is also an flow-stability indicator. The correspondance between Ri values and atmospheric stability, bearing in mind the previous paragraph discussion, is the following:

- $Ri > 0$ $\rightarrow$ Stable condition,

- $R \approx 0$ $\rightarrow$ Neutral condition,

- $Ri < 0$ $\rightarrow$ Unstable condition.

Fig. 3.10 and 3.11 show a comparison of the wind-velocity results and the Richardson number value at every time step. At a first glance, it can be seen that the highest Ri values (stable atmospheric conditions) occur during the hours of the day and the lowest ones, during the night (with some exceptions). Although, no large corraltion to larger or smaller observation-computation errors can be found, in the *Carcaixent* case, the Richardson number peak (23/07/11 at $6h$), i.e. the most stable conditions, occurs simultaneously to the highest match between computed and observed values.

Fig. 3.12 and 3.13 show a comparison of the wind-direction results and the Richardson number value at every time step. As in the wind-velocity case, no significant correlation between Richardson number and computed-observed values mismatch is found, except for the *Carcaixent* case, in which the Richardson number peak (23/07/11 at $6h$) occurs simultaneously to one of the largest wind direction errors.
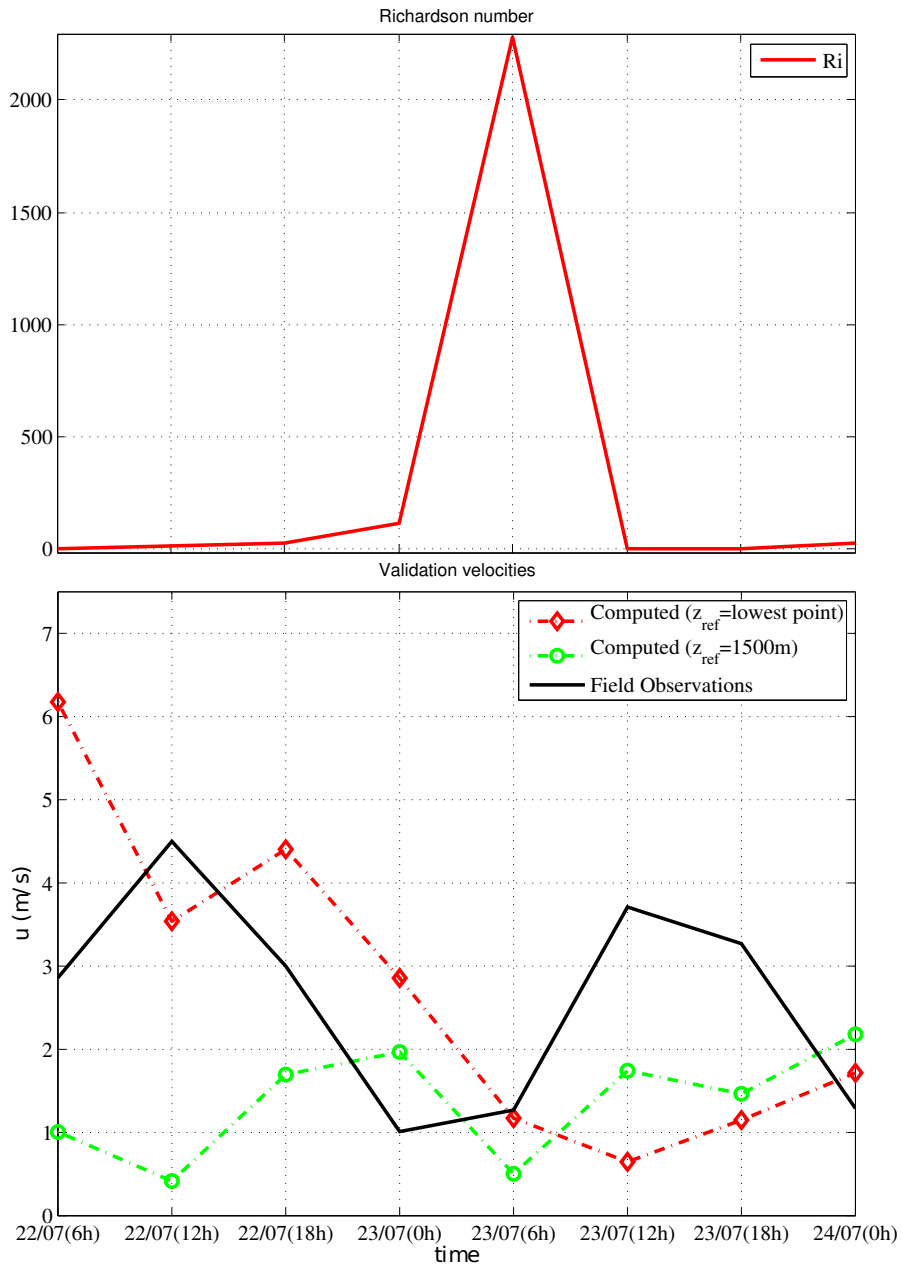
Figure 3.10: Richardson number comparison to wind-velocity results in *Carcaixent*.
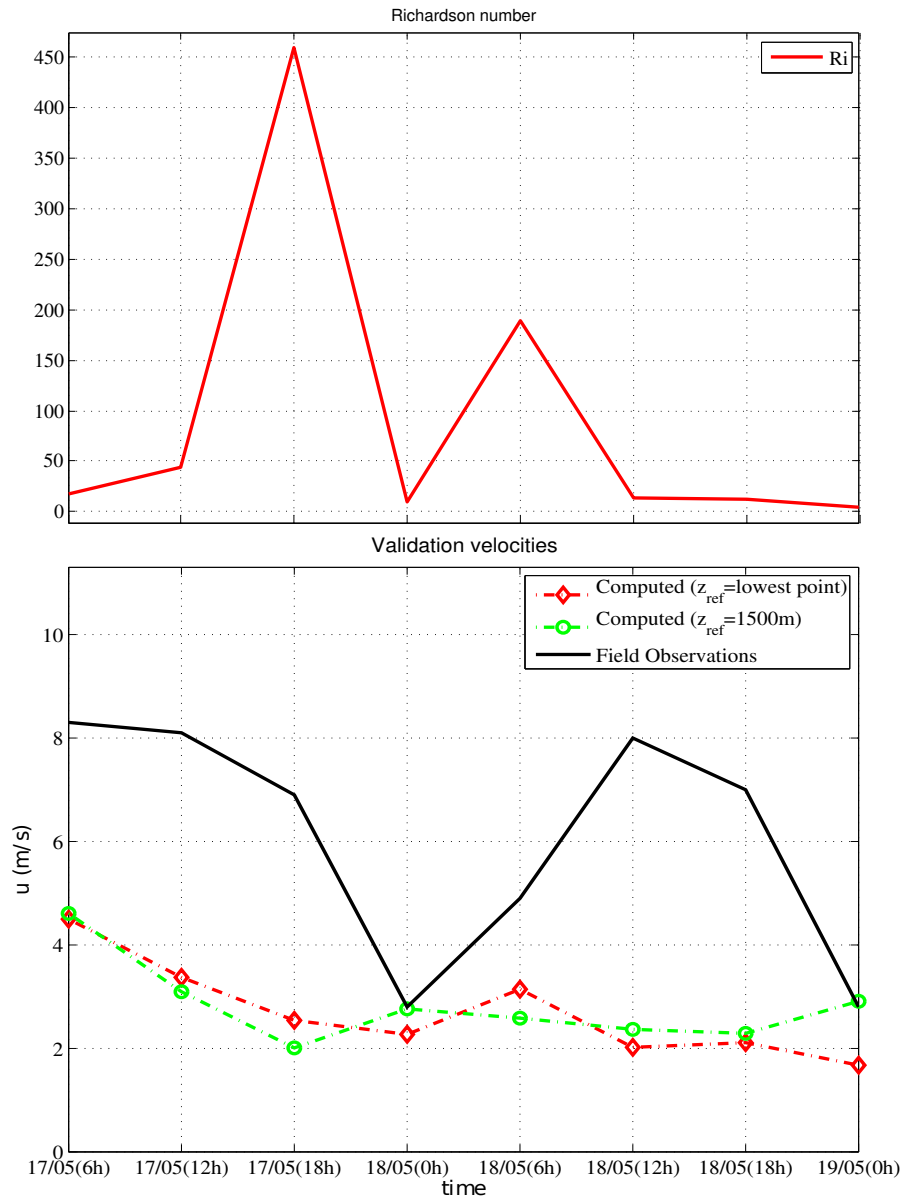
Figure 3.11: Richardson number comparison to wind-velocity results in *Wideûmont*.
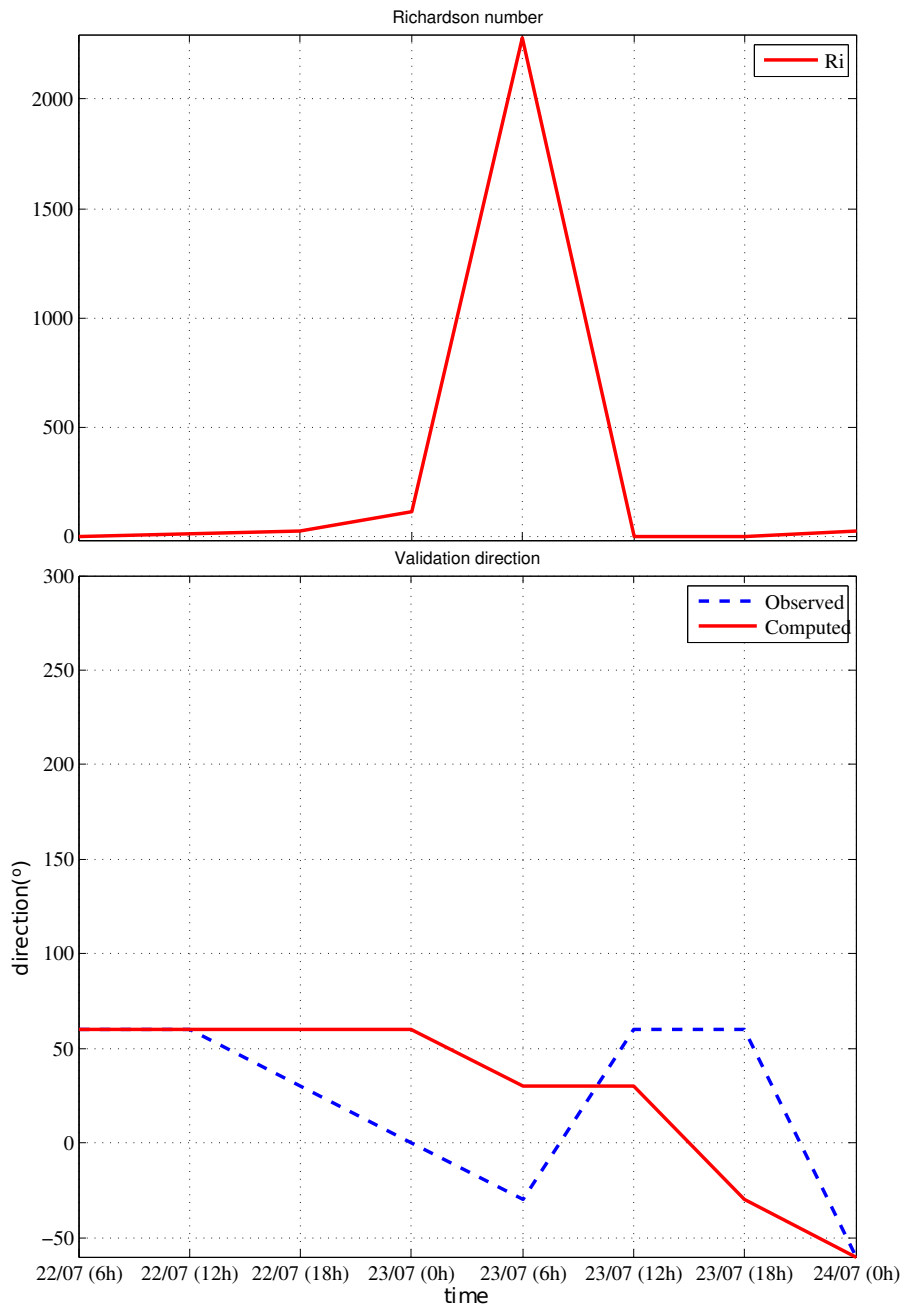
Figure 3.12: Richardson number comparison to wind-direction results in *Carcaixent*.
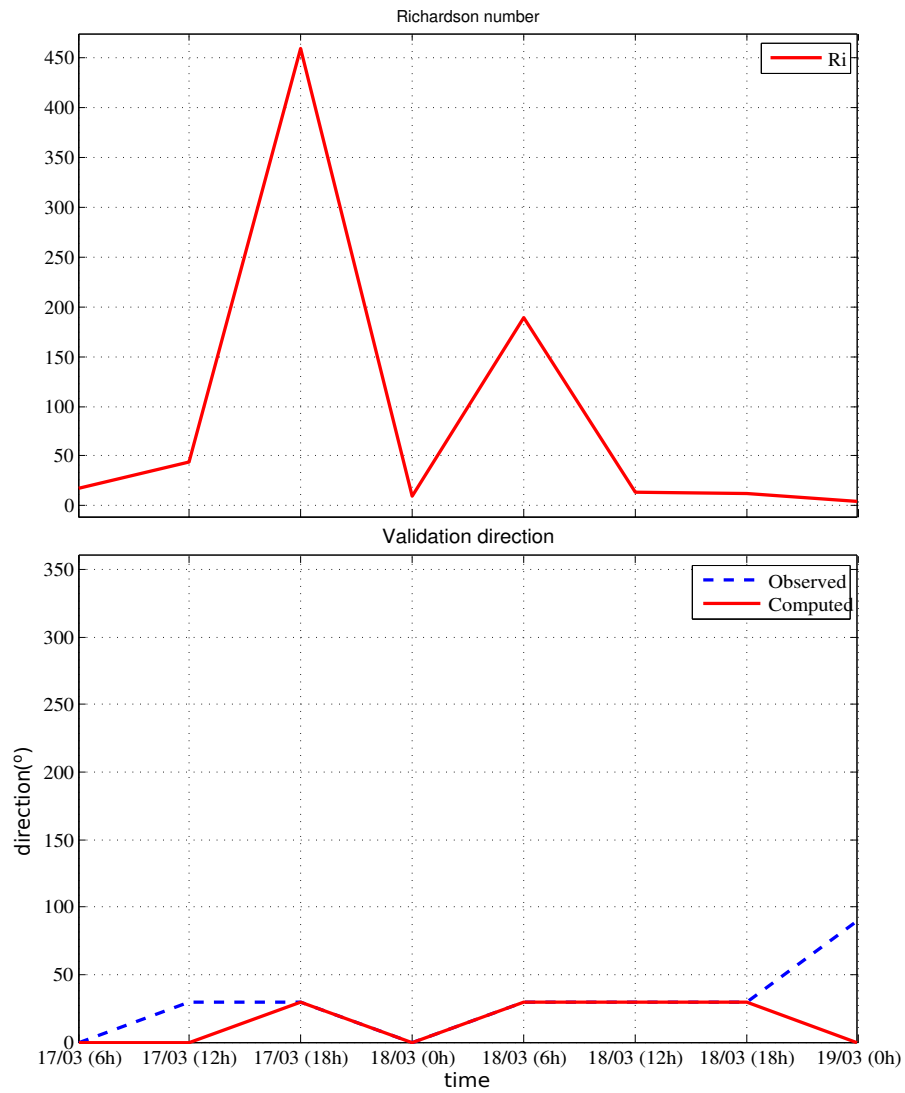
Figure 3.13: Richardson number comparison to wind-direction results in *Wideûmont*.

To sum up with respect to the results obtained, they are below the acceptance threshold when it comes to direct applications to the wind-engineering industry. This was expectable as, although the downscaling techniques have existed for decades, in this case the gap between the scales of the two models used is by far larger than the usual one, which represents the most innovative asset of this project.

Nevertheless, despite the bad results, as some trends are eventually detected, the work here explained is though to be the foundation of further research in the same direction, leading to the possible development of a whole new numerical model oriented to short-term wind-energy-resources prediction tool. Further discussion on this topic can be found in Sec. 4.3.

Chapter 4

Conclusions

This project consists of two main parts: the setup of *WAsP* in order to obtain a wind atlas of two regions, in Northern and Southern Europe, respectively, and the development and subsequent test of a downscaling tool to use it to downscale *NCEP/NCAR Reanalysis Data 1*.

4.1 Wind atlas

The *WAsP* model was set up and run in order to obtain a wind atlas of two regions of Europe in the first phase of this project. For this, data had to be provided on terrain topography, terrain roughness and wind climate of the region under study (no information on shelter produced by obstacles was provided, as they were modeled as roughness). The topography data was obtained out of *GTOPO30* ([16]) and converted to vector format by means of GIS applications. The roughness data was estimated out of *CORINE Land Cover* maps ([17]), associating an equivalent roughness length to every land-use code. Wind climate data was directly imported from the European Wind Atlas ([7]).

Despite the simplifications, the results obtained were generally good (relative errors under 7% extrapolating at distances above $100km$) except for those cases of coastal areas and islands (where offshore conditions exert an important bias on the estimates) or widely-separated stations.

4.2 Downscaling tool

A downscaling tool to refine *NCEP/NCAR Reanalysis Data 1* using *WAsP*-wind-climate data was proposed in the second phase of this project. For this the most relevant data of both models had to be selected. In the *NCEP/NCAR Reanalysis Data 1* case, they happened to be the wind velocity horizontal components, as the final goal of the project

was downscaling wind direction and velocity, and the geopotential height, which was used to convert the vertical coordinates from pressure levels to geometric height. Other conversions had to be applied to the *NCEP/NCAR Reanalysis Data 1*, such as time conversion from hours after 1948 to date format, scale factors, offset corrections, etc.

Out of *WAsP*, it was determined that, after running the model, the necessary data for the downscaling tool were the predicted wind climate profiles of the point under study, which have to be obtained out of the model GUI by hand.

Using the afore-mentioned data, an equation was found to combine them in order to finally obtain time-marching refined wind velocity and direction profiles. The downscaling process was automatized by means of a *MatLab* routine (which can be found in Appx. B) and validated using observed meteorological data in two stations in Europe: *Carcaixent* (València) and *Wideûmont* (Belgium). A large mismatch between the results concerning wind velocities was found, although the main trends were eventually followed by the model. As regards wind direction, better results were achieved.

The afore-mentioned development of new downscaling methods, according to several sources, such as [2], opens up great capabilities to apply mesoscale model data in a more sophisticated way and with higher resolutions, even for users with no background knowledge on CFD, which is likely the key of *WAsP*'s success.

The possibility of using global-scale NWP models to feed smaller-scale models opens up a wealth of possibilities, not only for short-term wind-energy-production prediction, as in the case of this project. This, in a near future, when computational resources are more powerful, numerical models more accurate and downscaling techniques more reliable, can provide good-quality estimates which are necessary in a lot cases. E.g. for promoting wind-energy programs in underdeveloped countries, where reliable time-series do not exist or their spatial coverage is too poor. Even in developed countries, such development will be an asset, as meteorological obseravation time-series have to be generally purchased to institutions and are gradually getting more expensive.

4.3 Recommendations

At last, a future work proposal may be outlined. As mentioned in the previous section, a mismatch between computed and observed wind velocity evolution was found, although the main trends were eventually followed. For this reason, it is important finding out the reason of this mismatch in order to figure out how to reduce the offset and the scale factor that makes observed and computed values different (i.e. calibrating the model). As regards wind velocity, since computed values tend in most of cases to underestimate the observations in both the wind map (*WAsP*) and the downscaling tool and the same *WAsP* data were used in both computations, this is likely the source of most of the error.

Therefore, improving the simulations with *WAsP* would be an asset. For this, better elevation and roughness maps could be used and an in-situ description of the obstacles surrounding the points under study could be performed.

Another action which would likely reduce errors would be refining *NCEP/NCAR Reanalysis Data 1* by means of *WRF* or a similar model. In this case, the latter model would be used as an intermediate step in the whole downscaling chain. Under a scheme *NCEP/NCAR Reanalysis Data 1*→*WRF*→*WAsP* a more gradual scale reduction, both in time and space, would likely improve results.

Also the whole downscaling method may be extended to the use of *NCEP/NCAR Reanalysis Data 1* from more than one point simultaneously, as other downscaling tools do (e.g. *KAMM/WAsP Method*, see [6]). It would be interesting finding out if some statistically-weighted system would yield better results.

In addition, the same method could be applied to other global datasets. According to [14], the global dataset used in this project (*NCEP/NCAR Reanalysis Data 1*) show significative time inconsistencies for some grid points of the Earth which, in some cases, affect drastically the energy production estimates, leading to errors up to 14% with respect to more consistent datasets, such as *MERRA*–grid data. As *NCEP/NCAR Reanalysis Data 1*, the *ECMWF Reanalysis Dataset* (published by *European Center for Medium-Range Weather Forecasts*) is also freely available for research purposes, but significatively more consistent, although their use is not as wide. Hence, developing a similar downscaling protocol to refine *ERA* data using *WAsP*, *openWind* or *WindPRO* data for wind-energy assessment purposes would be a both useful and challenging task.

Bibliography

[1] Landberg, L., Mortensen, N.G., Dellwik, E., Badger, J. Corbett, J.-F., Myllerup, L. and Rathmann, O. (2006), "Long-term (1-20 years) prediction of wind resources (WAsP)", in: *VKI Lecture Series*, February 23th, Von Karman Institute for Fluid Dynamics, Sint-Genesius-Rode (Belgium).

[2] Badger, J., Guo, Larsen, X.G., Mortensen, N..G., Hahmann, A., Hansen, J.C. and Joergensen, H.E. (2010), "A universal mesoscale to miscroscale modelling interface tool", in: *European Wind Energy Conference and Exhibition (EWEC)*, April 20th – 23th, European Wind Energy Association (EWEA), Warsaw (Poland).

[3] de Rooy, W. and Kok, K., (2002), *On the use of physical and statistical downscaling techniques for NWP model output*, Koninklijk Nederlands Meteorologisch Instituut, De Bilt (Holland).

[4] Landberg, L., Giebel, G., Madsen, H., Nielsen, T.S. and Nielsen, H.A. (2006), "Short-term (30 min–72 hrs) prediction for power output from wind farms", in: *VKI Lecture Series*, February 23th, Von Karman Institute for Fluid Dynamics, Sint-Genesius-Rode (Belgium).

[5] Verkaik, J.W., A.J.M. Jacobs, A.B.C. Tijm and J.R.A. Onvlee (2006), "Local wind speed estimation by physical downscaling of weather model forecasts", *Journal of Wind Engineering and Industrial Aerodynamics*.

[6] Frank, P.F., Rathmann, O., Mortensen, N.G., Landberg, L. (2001), *The Numerical Wind Atlas – the KAMM/WAsP Method*, Risø National Laboratory, Roskilde (Denmark).

[7] Troen, I. and Petersen, L. (1989), *European Wind Atlas*, Comission of European Communities – Directorate General for Science, Research and Development, Brussels (Belgium).

[8] Berge, E., Gravdahl, A.R., Schelling, J., Tallhaug and L., Undheim, O. (2006), "Wind in complex terrain. A comparison of WAsP and two CFD-models", in: *European Wind Energy Conference and Exhibition (EWEC)*, February 27th – March 2nd, European Wind Energy Association (EWEA), Athens (Greece).

[9] Bowen, A.J. and Mortensen, N.G. (2004), *WAsP prediction errors due to site orography*, Risø National Laboratory, Roskilde (Denmark).

[10] Walmsley, J.L., Troen, I., Lalas, D.P. and Mason, P.J. (1990), "Surface-layer flow in complex terrain: comparison of models and full-scale observations", *Boundary-layer Meteorology*, 52, p. 259-281.

[11] Bowen, A.J. and Mortensen, N.G. (1996), "Exploring the limits of WAsP, the Wind Atlas Analysis and Application Program", in: *European Wind Energy Conference and Exhibition (EWEC)*, May 20th – 24th, European Wind Energy Association (EWEA), Göteborg (Sweden).

[12] Wood, N. (1995), "The onset of separation in neutral, turbulent flow over hills", *Boundary-layer Meteorology*, 76, p. 137-164.

[13] Manning, J.P., Whiting, R.J., LeBlanc, M.P. and Hancock, P.E. (2005), "Optimising WAsP wind flow modelling for wind resource assessment around forested areas", in: *Conference for the Engineering Doctorate in Environmental Technology*, Brunel University, Brunel (United Kingdom).

[14] Liléo, S. and Petrik, O. (2011), "Investigation on the use of NCEP/NCAR, MERRA and NCEP/CFSR reanalysis data in wind resource analysis", in: *European Wind Energy Conference and Exhibition (EWEC)*, March 14th – 17th, European Wind Energy Association (EWEA), Brussels (Belgium).

[15] Houghton, J. (2002), *The physics of atmospheres* (3rd Ed.), Cambridge University Press, Cambridge (United Kingdom).

[16] EROS Data Center (EDC) (1996), *GTOPO30: Global 30 Arc-Second Elevation Data Set*, available at `http://edcdaac.usgs.gov/gtopo30/gtopo30.html` (accessed January 15th 2011).

[17] European Environment Agency (2000), *Corine Land Cover Maps*, available at `http://www.dataforwind.com/services/roughness_service.html` (accessed July 15th 2011), European Comission, Copenhagen (Denmark).

[18] Kalnay, E. et al. (1996), "The NCEP/NCAR 40-year reanalysis project", *Bulletin American Meteorology Society*, No. 77, p. 437-470.

[19] Malcorps H. (2009), *Vigilance Climatique* (in French "Climatic Survey"), Institut Royal Météorologique de Belgique, Brussels (Belgium).

[20] Orlanski, I. (1975), "A rational subdivision of scales for atmospheric processes", *Bulletin American Meteorology Society*, No. 56, p. 527-530.

[21] Vedel, H. (2000), *Conversion of WGS84 geometric heights to NWP model HIRLAM geopotential heights*, report number 00-04, Danish Meteorological Institut, Copenhagen (Denmark).

Appendices

Appendix A:

Data formats

This section deals with the different wind climate file-formats involved in the downscaling tool. Despite their file-extensions are different, all of them are plain text files and its absolute comprehension happens to be crucial in order to properly program the downscaling tool. Therefore, a short description of such files is carried out in the following sections.

NCEP/NCAR Reanalysis Data 1 format

The *NCEP/NCAR Reanalysis Data 1* may be downloaded in a wealth of possible formats according to the desired data subset. In the case under study, the data downloaded corresponds to horizontal and vertical wind velocities (U and V, respectively) at a single gridpoint, all of the 17 pressure levels and a single time step, e.g.:

```
netcdf u {
dimensions:
lon = 1 ;
lat = 1 ;
level = 17 ;
time = UNLIMITED ; // (1 currently)
variables:
float level(level) ;
level:units = "millibar" ;
level:actual_range = 1000.f, 10.f ;
level:long_name = "Level" ;
level:positive = "down" ;
level:GRIB_id = 100s ;
level:GRIB_name = "hPa" ;
level:axis = "Z" ;
float lat(lat) ;
lat:units = "degrees_north" ;
lat:actual_range = 50.f, 50.f ;
lat:long_name = "Latitude" ;
lat:standard_name = "latitude" ;
lat:axis = "Y" ;
float lon(lon) ;
lon:units = "degrees_east" ;
lon:long_name = "Longitude" ;
lon:actual_range = 5.f, 5.f ;
```

```
lon:standard_name = "longitude" ;
lon:axis = "X" ;
double time(time) ;
time:units = "hours since 1-1-1 00:00:0.0" ;
time:long_name = "Time" ;
time:actual_range = 17622606., 17622606. ;
time:delta_t = "0000-00-00 06:00:00" ;
time:standard_name = "time" ;
time:axis = "T" ;
short uwnd(time, level, lat, lon) ;
uwnd:long_name = "4xDaily U-wind" ;
uwnd:unpacked_valid_range = -125.f, 160.f ;
uwnd:actual_range = -13.5f, 14.2f ;
uwnd:units = "m/s" ;
uwnd:add_offset = 202.66f ;
uwnd:scale_factor = 0.01f ;
uwnd:missing_value = 32766s ;
uwnd:precision = 2s ;
uwnd:least_significant_digit = 1s ;
uwnd:GRIB_id = 33s ;
uwnd:GRIB_name = "UGRD" ;
uwnd:var_desc = "u-wind" ;
uwnd:dataset = "NMC Reanalysis" ;
uwnd:level_desc = "Multiple levels" ;
uwnd:statistic = "Individual Obs" ;
uwnd:parent_stat = "Other" ;
uwnd:valid_range = -32766s, -4266s ;

// global attributes:
:Conventions = "COARDS" ;
:title = "4x daily NMC reanalysis (2011)" ;
:history = "Tue May 24 02:55:52 2011: ncrcat -O -d level,10.000000,
1000.000000 -d lat,49.000000,51.000000 -d lon,4.000000,6.000000
-d time,545,545 /Datasets/ncep.reanalysis/pressure/uwnd.2011.nc
/Public/www/X193.191.4.173.143.2.55.51.nc\n",
"created 2011/01 by Hoop (netCDF2.3)" ;
:description = "Data is from NMC initialized reanalysis\n",
"(4x/day).  It consists of most variables interpolated to\n",
"pressure surfaces from model (sigma) surfaces." ;
:platform = "Model" ;
:references = "http://www.esrl.noaa.gov/psd/data/gridded/
data.ncep.reanalysis.html" ;
:nco_openmp_thread_number = 1 ;
```

```
data:

 level = 1000, 925, 850, 700, 600, 500, 400, 300, 250, 200, 150, 100, 70, 50,
    30, 20, 10 ;

 lat = 50 ;

 lon = 5 ;

 time = 17622606 ;

 uwnd =
  -19706,
  -19486,
  -19196,
  -19096,
  -19086,
  -18986,
  -18866,
  -18846,
  -18886,
  -19036,
  -19606,
  -19796,
  -20216,
  -20596,
  -21376,
  -21556,
  -21616 ;
}
```

Unlike other data format discussions, in this case, just a few parameters turn out to be actually relevant. Those are essentially the magnitude itself measured at the 17 pressure levels (from row 77 to 93). Nevertheless, these values have to be corrected to obtain the actual ones:

$$x_{act} = x_N \cdot \epsilon - \gamma \tag{A-1}$$

where x_{act} is the actual value, x_N is the non-corrected value provided by the *NCEP/N-CAR Reanalysis Data 1*, ϵ is the scale factor (row 41) and γ the offset (row 40).

A-3

WAsP data format

Observed wind climate

Observed wind climate data (henceforth, OWC) could be presented in two formats: as raw data (`.dat`) or statiscally represented in a histogram (`.tab`). In the first case, data consist on time series displayed in three columns (see the following example, where data are shown for January 1st 1983 at every $3h$):

```
83010100 5.0 239
83010103 4.1 214
83010106 4.1 207
83010109 4.3 213
83010112 5.5 238
83010115 4.2 193
83010118 4.5 202
83010121 4.7 202
...
```

where the rows have the following meaning:

1. Number string of year, month, day and hour,

2. Wind speed ($\frac{m}{s}$),

3. Wind direction (^{o}), e.g.:

As previously mentioned, OWC data can also be in their processed form (`.tab`), i.e. averaged conditions statistically represented in a histogram for every sector, e.g.:

```
Florennes, Belgium, 1975-81
       50.23          4.65          6.40
       12  1.0  0.0
    5.0, 7.0, 7.2, 7.6, 5.4, 6.2, 9.4,13.0,14.2,13.4, 7.1, 4.4,
 1, 141,  86, 128, 139, 149,  79,  56,  30,  46,  69,  92, 119,  83,
 2, 162, 119, 172, 298, 198,  84,  64,  45,  84, 115, 123, 154, 122,
 3, 233, 200, 211, 267, 201, 159, 130, 113, 132, 165, 162, 204, 170,
 4, 207, 205, 168, 135, 198, 233, 201, 160, 164, 160, 186, 204, 179,
 5, 141, 181, 128,  70, 131, 189, 208, 188, 166, 138, 165, 144, 157,
 6,  65, 114,  91,  39,  58, 118, 131, 143, 138, 115, 101,  87, 108,
 7,  32,  55,  61,  26,  47,  73, 105, 136, 118,  77,  72,  52,  81,
 8,  12,  24,  31,  16,  14,  37,  59,  97,  72,  72,  38,  26,  51,
```

A-4

```
 9,   6,   9,   7,   7,   5,  16,  24,  47,  38,  29,  27,   5,  23,
10,   1,   5,   3,   2,   0,   8,  14,  24,  16,  24,  18,   4,  13,
11,   0,   1,   1,   0,   0,   3,   5,  12,  14,  19,   6,   0,   7,
12,   0,   1,   0,   0,   0,   1,   2,   2,   8,   9,   5,   0,   3,
13,   0,   0,   0,   0,   0,   0,   1,   2,   2,   3,   1,   0,   1,
14,   0,   0,   0,   0,   0,   0,   0,   0,   1,   3,   1,   2,   1,
15,   0,   0,   0,   0,   0,   0,   0,   0,   2,   1,   2,   0,   1,
16,   0,   0,   0,   0,   0,   0,   0,   0,   0,   1,   0,   0,   0,
17,   0,   0,   0,   0,   0,   0,   0,   0,   0,   0,   0,   0,   0,
```

where the rows have the following meaning:

1 Identification of the meteorological station,

2 geographical coordinates, latitude and longitude (^{o}), and mast height (m a.g.l.),

3 number of sectors of wind directions, speed factor (column 1 is multiplied by this factor) and direction offset (wind roses are rotated by this parameter),

4 sectorwise wind direction frequency (wind rose),

5-21 according to the column:

   1 wind-speed bin upper limit,

   2-13 sectorwise wind direction frequency at the given velocity range (‰),

   14 mean wind velocity at the given velocity range (‰).

Regional wind climate

Regional wind climate data (henceforth, RWC) are essentially OWC data which have been "cleaned" of the site effects and are therefore extrapolable to compute wind climate conditions at any site of the domain (`.lib`), e.g. :

```
Florennes, Belgium 1975-81
  4  5 12
 0.000 0.030 0.100 0.400
 10.0  25.0  50.0 100.0 200.0
  4.7  6.3  7.1  7.3  6.4  6.0  8.2 11.7 13.7 13.7  9.6  5.4
 5.82, 6.27, 6.10, 4.80, 4.90, 6.67, 7.91, 8.85, 8.80, 8.00, 7.29, 6.64, 7.22,
 2.32, 2.48, 2.34, 1.83, 1.90, 2.46, 2.68, 2.81, 2.66, 2.25, 2.08, 2.17, 2.16,
 6.37, 6.86, 6.68, 5.26, 5.37, 7.30, 8.65, 9.68, 9.63, 8.76, 7.98, 7.27, 7.90,
 2.39, 2.56, 2.41, 1.88, 1.96, 2.54, 2.77, 2.90, 2.74, 2.32, 2.15, 2.24, 2.22,
 6.84, 7.37, 7.17, 5.65, 5.77, 7.83, 9.29, 10.4, 10.3, 9.40, 8.57, 7.81, 8.49,
 2.45, 2.63, 2.47, 1.93, 2.02, 2.61, 2.84, 2.98, 2.82, 2.38, 2.20, 2.30, 2.26,
 7.42, 7.99, 7.78, 6.12, 6.25, 8.50, 10.1, 11.3, 11.2, 10.2, 9.29, 8.47, 9.20,
 2.38, 2.55, 2.40, 1.87, 1.95, 2.53, 2.75, 2.88, 2.73, 2.31, 2.13, 2.22, 2.21,
 8.21, 8.85, 8.60, 6.75, 6.89, 9.40, 11.2, 12.5, 12.4, 11.3, 10.3, 9.36, 10.2,
 2.25, 2.41, 2.27, 1.77, 1.85, 2.39, 2.60, 2.73, 2.58, 2.19, 2.02, 2.10, 2.10,
  4.9  6.7  7.2  7.5  5.7  6.1  9.0 12.6 14.0 13.5  8.0  4.8
 3.98, 4.54, 4.11, 3.12, 3.74, 4.93, 5.66, 6.35, 6.04, 5.39, 5.03, 4.46, 5.04,
 1.97, 2.13, 1.85, 1.49, 1.76, 2.17, 2.28, 2.44, 2.17, 1.80, 1.78, 1.85, 1.87,
 4.77, 5.43, 4.93, 3.77, 4.49, 5.89, 6.76, 7.59, 7.23, 6.47, 6.03, 5.35, 6.05,
 2.12, 2.30, 2.00, 1.60, 1.90, 2.34, 2.47, 2.64, 2.34, 1.95, 1.92, 2.00, 2.00,
 5.51, 6.27, 5.71, 4.39, 5.20, 6.80, 7.80, 8.74, 8.34, 7.49, 6.99, 6.19, 7.00,
 2.38, 2.59, 2.25, 1.80, 2.13, 2.63, 2.77, 2.97, 2.63, 2.19, 2.16, 2.25, 2.21,
 6.53, 7.43, 6.77, 5.23, 6.18, 8.05, 9.23, 10.4, 9.88, 8.89, 8.30, 7.34, 8.31,
 2.54, 2.76, 2.40, 1.92, 2.27, 2.81, 2.95, 3.16, 2.81, 2.33, 2.30, 2.40, 2.33,
 8.13, 9.26, 8.43, 6.49, 7.68, 10.0, 11.5, 12.9, 12.3, 11.1, 10.3, 9.14, 10.3,
 2.42, 2.63, 2.29, 1.83, 2.17, 2.68, 2.82, 3.02, 2.68, 2.22, 2.19, 2.29, 2.24,
  5.0  6.9  7.2  7.6  5.5  6.2  9.2 12.9 14.2 13.5  7.4  4.5
 3.42, 4.00, 3.53, 2.72, 3.37, 4.35, 4.96, 5.54, 5.22, 4.63, 4.36, 3.83, 4.39,
 1.97, 2.16, 1.81, 1.52, 1.85, 2.19, 2.31, 2.42, 2.13, 1.76, 1.79, 1.90, 1.87,
 4.23, 4.94, 4.37, 3.37, 4.16, 5.37, 6.11, 6.83, 6.44, 5.73, 5.40, 4.73, 5.43,
 2.11, 2.31, 1.94, 1.63, 1.98, 2.34, 2.48, 2.59, 2.28, 1.89, 1.92, 2.03, 1.98,
 4.96, 5.78, 5.13, 3.98, 4.89, 6.28, 7.15, 7.98, 7.54, 6.73, 6.35, 5.55, 6.37,
 2.34, 2.56, 2.14, 1.80, 2.19, 2.59, 2.74, 2.87, 2.53, 2.09, 2.12, 2.25, 2.16,
 5.90, 6.87, 6.11, 4.77, 5.83, 7.47, 8.49, 9.48, 8.97, 8.03, 7.56, 6.61, 7.60,
 2.57, 2.81, 2.35, 1.98, 2.40, 2.85, 3.01, 3.15, 2.78, 2.30, 2.33, 2.47, 2.34,
 7.29, 8.49, 7.54, 5.87, 7.19, 9.23, 10.5, 11.7, 11.1, 9.90, 9.33, 8.16, 9.37,
 2.46, 2.69, 2.25, 1.90, 2.30, 2.73, 2.88, 3.02, 2.66, 2.20, 2.23, 2.37, 2.26,
```

```
   5.2  7.1  7.3  7.3  5.5  6.4  9.7 13.1 14.2 12.9  6.9  4.5
  2.75, 3.13, 2.71, 2.12, 2.78, 3.50, 3.97, 4.36, 4.06, 3.61, 3.40, 2.96, 3.46,
  2.01, 2.12, 1.78, 1.50, 1.90, 2.19, 2.32, 2.42, 2.10, 1.76, 1.79, 1.90, 1.87,
  3.62, 4.12, 3.58, 2.81, 3.67, 4.61, 5.22, 5.73, 5.34, 4.77, 4.49, 3.90, 4.56,
  2.13, 2.25, 1.89, 1.59, 2.02, 2.32, 2.46, 2.56, 2.23, 1.87, 1.90, 2.01, 1.97,
  4.37, 4.97, 4.33, 3.41, 4.43, 5.55, 6.28, 6.90, 6.45, 5.77, 5.43, 4.72, 5.51,
  2.31, 2.44, 2.05, 1.73, 2.19, 2.53, 2.67, 2.78, 2.42, 2.03, 2.06, 2.18, 2.12,
  5.26, 5.98, 5.22, 4.14, 5.34, 6.68, 7.55, 8.28, 7.75, 6.97, 6.56, 5.69, 6.65,
  2.63, 2.78, 2.34, 1.96, 2.50, 2.88, 3.05, 3.17, 2.76, 2.31, 2.35, 2.49, 2.37,
  6.44, 7.31, 6.38, 5.05, 6.53, 8.16, 9.23, 10.1, 9.48, 8.51, 8.01, 6.95, 8.12,
  2.54, 2.68, 2.26, 1.89, 2.40, 2.77, 2.93, 3.06, 2.66, 2.22, 2.26, 2.40, 2.29,
```

where the rows have the following meaning[1]:

  1 Identification of the meteorological station,

  2 number of roughness classes, height classes and sectors,

  3 characteristic roughness of every class (m),

  4 characteristic height of every class (m),

  5 sectorwise wind direction frequency (wind rose) in roughness class 1 terrains,

  6 sectorwise Weibull scale-parameter (A) for roughness class 1 and height class 1,

  7 sectorwise Weibull shape-parameter (k) for roughness class 1 and height class 1,

  8 sectorwise Weibull scale-parameter (A) for roughness class 1 and height class 2,

  9 sectorwise Weibull shape-parameter (k) for roughness class 1 and height class 2,

 10 sectorwise Weibull scale-parameter (A) for roughness class 1 and height class 3,

 11 sectorwise Weibull shape-parameter (k) for roughness class 1 and height class 3,

 12 sectorwise Weibull scale-parameter (A) for roughness class 1 and height class 4,

 13 sectorwise Weibull shape-parameter (k) for roughness class 1 and height class 4,

 14 sectorwise Weibull scale-parameter (A) for roughness class 1 and height class 5,

 15 sectorwise Weibull shape-parameter (k) for roughness class 1 and height class 5,

16-26 idem rows [5-15] for roughness class 2,

27-37 idem rows [5-15] for roughness class 3,

38-48 idem rows [5-15] for roughness class 4,

---

[1]from row 6 to 15 and respectively for other roughness classes, the last column corresponds to the sector-averaged conditions

Predicted wind climate

Predicted wind climate data (henceforth, PWC) contain wind resources and energy assessment at a given site (`.txt`). This is one of the possible outputs of *WAsP* and happens to be the most relevant file-format, e.g.:

```
'Dourbes' Turbine site
Produced on 30/05/11 at 15:11:37 by licenced user...

Settings
Hub Height a.s.l.: 10
X Co-ordinate: 613867
Y Co-ordinate: 5550015
Elevation a.s.l.: 210

Site effects
Sector Roughness Obst. Orography
# ang.[deg] ch ref.[m] sp[%] sp[%] sp[%] tu[deg] RIX dRIX
1 0 0 0.395 0.00 0.00 -4.11 0.4 0.0
2 30 0 0.398 0.00 0.00 -2.35 1.4 0.0
3 60 0 0.400 0.00 0.00 -0.05 1.0 0.0
4 90 0 0.347 0.00 0.00 0.52 -0.4 0.0
5 120 1 0.241 -7.81 0.00 -1.19 -1.4 0.0
6 150 1 0.218 -9.34 0.00 -3.50 -1.0 0.0
7 180 1 0.204 -9.94 0.00 -4.09 0.4 0.0
8 210 1 0.198 -10.43 0.00 -2.34 1.4 0.0
9 240 1 0.218 -9.04 0.00 -0.05 1.0 0.0
10 270 1 0.257 -6.86 0.00 0.52 -0.4 0.0
11 300 1 0.309 -4.21 0.00 -1.18 -1.4 0.0
12 330 0 0.386 0.00 0.00 -3.50 -1.0 0.0
All                 0.0

Wind and Power
Sector Wind Climate Power
# ang.[deg] freq.[%] W-A[m/s] Weibull-k U[m/s] power[W/m2] AEP[GWh] wake[%]
1 0 -95.00 2.6 2.01 2.34 15 --
2 30 -93.03 3.1 2.12 2.70 22 --
3 60 -92.50 2.7 1.79 2.42 19 --
4 90 -92.43 2.2 1.51 2.00 13 --
5 120 -94.42 2.8 1.88 2.45 18 --
6 150 -93.84 3.4 2.19 3.01 29 --
7 180 -90.90 3.8 2.31 3.41 40 --
8 210 -87.23 4.3 2.42 3.84 56 --
```

```
9 240 -85.44 4.2 2.12 3.69 55 --
10 270 -86.56 3.7 1.76 3.28 48 --
11 300 -93.04 3.4 1.79 3.00 36 --
12 330 -95.62 2.9 1.90 2.55 20 --
All (3.4) (1.86) 3.06 36 --

User Corrections
Sector Corections
# ang.[deg] speed[%] turn[deg]
1 0 0.00 0
2 30 0.00 0
3 60 0.00 0
4 90 0.00 0
5 120 0.00 0
6 150 0.00 0
7 180 0.00 0
8 210 0.00 0
9 240 0.00 0
10 270 0.00 0
11 300 0.00 0
12 330 0.00 0
```

Unlike previous data format discussions, in this case, just a few parameters turn out to be relevant. Those are the following: from line 5 to 8, the hub height, the geographic coordinates and the terrain elevation above the sea level are provided. In columns 4 and 5 from row 31 to 42, the sectorwise Weibull distribution parameters are respectively provided.

Appendix B:

MatLab routine

This section reproduces the *MatLab* routine thanks to which the downscaling process described in the present project can be automatized. For a theoretical discussion on the data used and the operations performed, see Sec. 2.4.

In order to execute the downscaling process in a more orderly way, it was split in a series of subroutines featuring both *MatLab* and *Linux* codes. The hierarchy of the subroutines involved in the downscaling tool is the following[2]:

Table B-1: Downscaling Matlab-subroutines tree

Directory	File	Type
./	*master.m*	*MatLab*
./ncar/	*extractdata.sh*	*Linux*
	ncarprofile.m	*MatLab*
./wasp/	*clearhyphens.sh*	*Linux*
	waspprofile.m	*MatLab*
./downscaling/	*downscaling.m*	*MatLab*
./validation/	*validation.m*	*MatLab*

The input files regarding *WAsP* profiles (wind climate at 20 heights), the *NCEP/N-CAR Reanalysis Data 1* (wind climate for the 8 timesteps) and the observed wind velocity and directions during the 8 timestops, must be introduced in the following directories:

– *w*.txt* (*WAsP* input) in *./wasp/*,

– *u.nc*, *v.nc* and *z.nc* (*NCEP/NCAR Reanalysis Data 1* input) in *./ncar/n*/*,

– *observations* (meteorological station observations) in *./observations/*,

The final results provided by the application are plots of the sectorwise *WAsP* profiles, plots of the *NCEP/NCAR Reanalysis Data 1* profiles for every time step, plots of the downscaled profiles for every time step and a graphic comparison of wind velocity and direction between computed and observed values. They are saved in `.pdf` in different directories according to the characteristics of the data.

---

[2]The functions concerning time conversion are the following: *converthourad2date.m*, *daysinmonth.m*, *istime.m*, *sec2hms.m*, *date2jd.m*, *daysinyear.m*, *jd2date.m*, *unixsecs2date.m*, *date2mjd.m*, *easterday.m*, *jd2jdate.m*, *weekofyear.m*, *date2unixsecs.m*, *hms2days.m*, *jd2mjd.m*, *weeksinyear.m*, *dayofmonth.m*, *hms2sec.m*, *jdate2jd.m*, *yearnum.m*, *dayofweek.m*, *isdate.m*, *mjd2date.m*, *dayofyear.m*, *isjdate.m*, *mjd2jd.m*, *days2hms.m*, *isleapyear.m*, *monthofyear.m*. Those routines are in the directory *./ncar/timeconversion/*, although they are not shown for practical reasons.

master.m

```
 1  clear
 2  clc
 3
 4  %%% LOAD AND PROCESS NCEP/NCAR REANALYSIS DATA %%%
 5
 6  cd ncar
 7  ncarprofile
 8  cd ..
 9
10  %%% LOAD AND PROCESS AND LOAD WAsP DATA %%%
11
12  cd wasp
13  waspprofile
14  cd ..
15
16  %%% DOWNSCALING %%%
17
18  cd downscaling
19  downscaling
20
21  %%% VALIDATION %%%
22
23  cd validation
24  validation
```

extractdata.sh

```
1  cd n1
2  ncdump z.nc > z &
3  ncdump u.nc > u &
4  ncdump v.nc > v &
5  cd ..
6  cd n2
7  ncdump z.nc > z &
8  ncdump u.nc > u &
9  ncdump v.nc > v &
10 cd ..
11 cd n3
12 ncdump z.nc > z &
13 ncdump u.nc > u &
14 ncdump v.nc > v &
15 cd ..
16 cd n4
17 ncdump z.nc > z &
18 ncdump u.nc > u &
19 ncdump v.nc > v &
20 cd ..
21 cd n5
22 ncdump z.nc > z &
23 ncdump u.nc > u &
24 ncdump v.nc > v &
25 cd ..
26 cd n6
27 ncdump z.nc > z &
28 ncdump u.nc > u &
29 ncdump v.nc > v &
30 cd ..
31 cd n7
32 ncdump z.nc > z &
33 ncdump u.nc > u &
34 ncdump v.nc > v &
35 cd ..
36 cd n8
37 ncdump z.nc > z &
38 ncdump u.nc > u &
39 ncdump v.nc > v &
40 cd ..
```

ncarprofile.m

```
1  %%% INPUT DATA %%%
2
3  latitude=input('Introduce latitude of point under study in degrees: ');
4
5  cd ..
6  cd wasp
7  elevation=dlmread('w10.txt',':',[7 1 7 1]); % elevation of terrain above
      sea level
8  cd ..
9  cd ncar
10
11 %%% IMPORT FILE %%%
12
13 %%% extract %%%
14 system('sh extractdata.sh');
15 disp('Extracting NCEP/NCAR Reanalysis Data, please wait...')
16 pause(4) %this is to avoid that MatLab calls 'z', 'u' and 'v' before
      extractdata.sh has finished extracting them! (If problems arise,
      increase the pause duration).
17 clc
18
19 %%% LOOP STARTS FOR EACH TIME STEP %%%
20
21 for x=1:8;
22
23 accessdirectory=strcat('cd n',num2str(x));
24 eval(accessdirectory);
25
26 %%% u %%%
27 ncar_zfirst=dlmread('z',',',[76,0,91,0]);ncar_zlast=dlmread('z',';'
      ,[92,0,92,0]);ncar_z=[ncar_zfirst;ncar_zlast];
28 %%% v %%%
29 ncar_ufirst=dlmread('u',',',[76,0,91,0]);ncar_ulast=dlmread('u',';'
      ,[92,0,92,0]);ncar_u=[ncar_ufirst;ncar_ulast];
30 %%% z %%%
31 ncar_vfirst=dlmread('v',',',[76,0,91,0]);ncar_vlast=dlmread('v',';'
      ,[92,0,92,0]);ncar_v=[ncar_vfirst;ncar_vlast];
32 %%% t %%%
33 timeu=dlmread('u','=',[73,1,73,1]);timev=dlmread('u','=',[73,1,73,1]);timez
      =dlmread('u','=',[73,1,73,1]);
34 if timeu==timev & timev==timez;time=timeu;else disp('ERROR: mismatch
      between several files time range!');end
35
36 clear ncar_zfirst;clear ncar_ufirst;clear ncar_vfirst;clear ncar_zlast;
      clear ncar_ulast;clear ncar_vlast;
37 clear timeu;clear timev;clear timez;
38
39 %%% CHECKING FILE FORMAT %%%
40
41 numberoflongitudesu=dlmread('u','=',[2,1,2,1]);
42 numberoflongitudesv=dlmread('v','=',[2,1,2,1]);
```

```
43  numberoflongitudesz=dlmread('z','=',[2,1,2,1]);
44  if numberoflongitudesu==numberoflongitudesv & numberoflongitudesv==
        numberoflongitudesz;
45  numberoflongitudes=numberoflongitudesu;
46  else disp('ERROR: mismatch between several files number of points!');
47  end;
48  if numberoflongitudes~=1;disp('Number of points must be 1!');end;
49
50  numberoflatitudesu=dlmread('u','=',[3,1,3,1]);
51  numberoflatitudesv=dlmread('v','=',[3,1,3,1]);
52  numberoflatitudesz=dlmread('z','=',[3,1,3,1]);
53  if numberoflatitudesu==numberoflatitudesv & numberoflatitudesv==
        numberoflatitudesz;
54  numberoflatitudes=numberoflatitudesu;
55  else disp('ERROR: mismatch between several files number of points!');
56  end;
57  if numberoflatitudes~=1;disp('Number of points must be 1!');end;
58
59  numberofpressurelevelsu=dlmread('u','=',[4,1,4,1]);
60  numberofpressurelevelsv=dlmread('v','=',[4,1,4,1]);
61  numberofpressurelevelsz=dlmread('z','=',[4,1,4,1]);
62  if numberofpressurelevelsu==numberofpressurelevelsv &
        numberofpressurelevelsv==numberofpressurelevelsz;
63  numberofpressurelevels=numberofpressurelevelsu;
64  else disp('ERROR: mismatch between several files number of pressure levels!
        ');
65  end;
66  if numberofpressurelevels~=17;disp('Number of pressure levels must be 17!')
        ;end;
67
68  clear numberoflongitudesu;clear numberoflongitudesv;clear
        numberoflongitudesz;clear numberoflongitudes;
69  clear numberoflatitudesu;clear numberoflatitudesv;clear numberoflatitudesz;
        clear numberoflatitudes;
70  clear numberofpressurelevelsu;clear numberofpressurelevelsv;clear
        numberofpressurelevelsz;clear numberofpressurelevels;
71
72  %%% PROFILES COMPUTATION %%%
73
74  %%% time %%%
75  cd ..
76  cd timeconversion
77  converthourad2date;
78  cd ..
79  eval(accessdirectory);
80
81  %%% g %%%
82  g0=9.780327*(1+0.00193185138639*(sind(latitude))^2)/(sqrt
        (1-0.00669437999013*(sind(latitude))^2));
83
84  %%% r %%%
85  a=6378137;b=6356752;
```

B-5

```matlab
86  r=sqrt((((((a^2)*cosd(latitude))^2)+((((b^2)*sind(latitude))^2)))/(((((a^1)*
        cosd(latitude))^2)+((((b^1)*sind(latitude))^2)))));
87
88  %%% z %%%
89  scalez=dlmread('z','=',[40,1,40,1]);
90  offsetz=dlmread('z','=',[39,1,39,1]);
91  zg=(ncar_z.*scalez)+offsetz; % potential height
92  G=g0*r/9.80665;
93  H=zg.*G./(r+zg); % geometric height
94
95  for firstpoint=1:17;
96  if H(firstpoint,1)-elevation>0;break;end;
97  end;
98
99  z=H(firstpoint:17,1)-elevation;
100
101  %%% u %%%
102  scaleu=dlmread('u','=',[40,1,40,1]);
103  offsetu=dlmread('u','=',[39,1,39,1]);
104  u=(ncar_u(firstpoint:17,1).*scaleu)+offsetu;
105
106  %%% v %%%
107  scalev=dlmread('v','=',[40,1,40,1]);
108  offsetv=dlmread('v','=',[39,1,39,1]);
109  v=(ncar_v(firstpoint:17,1).*scalev)+offsetv;
110
111  %%% u+v %%%
112  uv=((u.^2)+(v.^2)).^0.5;
113  clear G;clear g0;
114
115  %%% k %%%
116  dir=[atand(v./u)];
117
118  for index=1:17+1-firstpoint;
119  if dir(index,1)>75 & dir(index,1)<=105;sector(index,1)=1;end;
120  if dir(index,1)>45 & dir(index,1)<=75;sector(index,1)=2;end;
121  if dir(index,1)>15 & dir(index,1)<=45;sector(index,1)=3;end;
122  if dir(index,1)>-15 & dir(index,1)<=15;sector(index,1)=4;end;
123  if dir(index,1)>-45 & dir(index,1)<=-15;sector(index,1)=5;end;
124  if dir(index,1)>-75 & dir(index,1)<=-45;sector(index,1)=6;end;
125  if dir(index,1)>-105 & dir(index,1)<=-75;sector(index,1)=7;end;
126  if dir(index,1)>-135 & dir(index,1)<=-105;sector(index,1)=8;end;
127  if dir(index,1)>-165 & dir(index,1)<=-135;sector(index,1)=9;end;
128  if dir(index,1)>=-180 & dir(index,1)<=-165;sector(index,1)=10;end; % sector
         10
129  if dir(index,1)>165 & dir(index,1)<=180;sector(index,1)=10;end;      % is
         split
130  if dir(index,1)>135 & dir(index,1)<=165;sector(index,1)=11;end;
131  if dir(index,1)>105 & dir(index,1)<=135;sector(index,1)=12;end;
132  end;
133
134  %%% limit %%%
135  limit=[200,200];
```

```
136  aux2=[−1000,1000];
137
138  %%% WRITE TO OUTPUT TEXT FILE %%%
139
140  filename=strcat('output_ncar',num2str(x));
141  [LOG,LOGerror]=fopen('output_ncar','w');
142  fprintf(LOG,'Wind velocity profile');fprintf(LOG,'\n');
143  fprintf(LOG,'*** date *** \n');fprintf(LOG,datencar);fprintf(LOG,'\n');
144  fprintf(LOG,'*** u *** \n');fprintf(LOG,'%−0.1f ',u);fprintf(LOG,'\n');
145  fprintf(LOG,'*** v *** \n');fprintf(LOG,'%−0.1f ',v);fprintf(LOG,'\n');
146  fprintf(LOG,'*** u+v *** \n');fprintf(LOG,'%−0.1f ',uv);fprintf(LOG,'\n');
147  fprintf(LOG,'*** sector *** \n');fprintf(LOG,'%−0.0f ',sector);fprintf(LOG,
         '\n');
148  fprintf(LOG,'*** z *** \n');fprintf(LOG,'%−0.0f ',z);fprintf(LOG,'\n');
149  fclose(LOG);
150  clear filename;
151
152  %%% PLOT VELOCITY PROFILES %%%
153
154  filename=strcat('ncarprof',num2str(x),'.pdf');
155  plot(u,z,'rx','LineWidth',2);hold on;
156  plot(v,z,'bo','LineWidth',2);hold on;
157  plot(uv,z,'k','LineWidth',1);hold on;
158  plot(aux2,limit,'k—','LineWidth',1),grid,title(datencar);legend('u(x)','v(
         y)','sqrt(u^2+v^2)'),options={'interpreter','latex','Fontsize',12};
         xlabel('$u$ (m/s)',options{:}),ylabel('$z$ (m)',options{:}),set(gca,'
         XLim',[min([min(u),min(v)]),max(uv)],'YLim',[0,max(z)]),set(gca,'
         FontSize',12,'FontName','Times'),saveas(gcf,filename);hold off;
159
160  clc;
161
162  if z(1,1)<0;
163  disp('WARNING! Terrain elevation higher than lower point of NCEP/NCAR
         Reanalysis Data velocity profile!');
164  end;
165
166  confirmation=['NCEP/NCAR: Plot of ',num2str(datencar),' saved as ',filename
         ,' successfully!'];
167  disp(confirmation) %to crop pdf or other images in LaTeX use command "trim
         "!
168
169  clear secs;clear aux1;clear aux2;clear a;clear b;clear LOG;clear LOGerror;
         clear dir;clear ans;clear limit;clear offset*;clear scale*;clear year;
         clear month;clear day;clear hour;clear minute;clear second;clear
         confirmation;clear options;clear index;clear ncar*;clear time*;clear r;
         clear x;clear zg; clear accessdirectory;
170
171  cd ..
172
173  end;
```

clearhyphens.sh

```
1  cat $1 | sed -e "s/-  //g" > $2
```

waspprofile.m

```matlab
1  clc
2
3  %%% LOAD HEIGHTS %%%
4
5  for i=10:10:200
6      filename=strcat('w',num2str(i),'.txt');
7      z(i/10,1)=dlmread(filename,':',[4 1 4 1]);if z(i/10,1)~=i;disp('ERROR!
          WAsP profiles not defined in (10m,200m) every 10m!');end;
8  end;
9  %clear i;clear filename;
10
11 %%% LOAD WEIBULL PARAMETERS %%%
12
13 for i=10:10:200;
14     filename=num2str(i);
15     scriptcall=strcat('./cleanhyphens.sh w',filename,'.txt w',filename,'
          nohyph.txt');
16     system(scriptcall);
17 end;
18 %clear i;clear filename; clear scriptcall;clear ans;
19
20 %%% k %%%%
21
22 for i=10:10:200 %height
23     filename=strcat('w',num2str(i),'nohyph.txt');
24     k(:,i/10)=dlmread(filename,'\t',[30 4 41 4]);
25 end;
26 clear i;clear filename;
27
28 %%% L %%%%
29
30 for i=10:10:200 %height
31     filename=strcat('w',num2str(i),'nohyph.txt');
32     L(:,i/10)=dlmread(filename,'\t',[30 5 41 5]);
33 end;
34 clear i;clear filename;
35
36 %%% U %%%
37
38 for i=1:1:20; %height
39     for n=1:1:12;
40     U(n,i)=L(n,i)*gamma(1+(1/k(n,i)));
41     end;
42 end;
43
44 %clear i;clear filename;clear n;
45
46 %%% WRITE TO OUTPUT TEXT FILE %%%
47
48 [LOG,LOGerror]=fopen('output_wasp','w');
49 fprintf(LOG,'Wind velocity profiles\n');
```

B-9

```matlab
50  fprintf(LOG,'*** U *** (row=sector; column=height) \n');
51
52  for n=1:12;
53  fprintf(LOG,'%-0.2f ',U(n,:));fprintf(LOG,'\n');
54  end;
55
56  fprintf(LOG,'*** z *** \n');fprintf(LOG,'%-0.0f ',z);fprintf(LOG,'\n');
57  fclose(LOG);clear LOG;clear LOGerror;
58
59  %%% WIND VELOCITY PROFILES %%%
60
61  for n=1:12;
62  titletext=strcat('Velocity profile - sector ',num2str(n));
63  filename=strcat('waspprofile_sect ',num2str(n),'.pdf');
64  plot(U(n,1:20),z,'b','LineWidth',2),grid,title(titletext);options={'
        interpreter','latex','Fontsize',12};xlabel('$u (m/s)$',options{:}),
        ylabel('$z(m)$',options{:}),set(gca,'XLim',[0,max(U(n,1:20))],'YLim'
        ,[0,max(z)]),set(gca,'FontSize',12,'FontName','Times'),saveas(gcf,
        filename);
65  message=strcat('WAsP: Plot for sector ',num2str(n),' saved as ',filename,'
        successfully!');
66  disp(message);
67  end;
68
69  system('rm w*nohyph.txt');
```

downscaling.m

```matlab
1  cd ..
2  clc;disp('Starting data downscaling process, please wait...')
3  pause(1);
4
5  for y=1:8;
6  cd ncar
7  accessdirectory=strcat('cd n',num2str(y));
8  eval(accessdirectory); clear accessdirectory;
9
10 %%% sector downscaled data at reference height %%%
11 sector_ref(y,1)=dlmread('output_ncar',' ',[10,0,10,0]);
12
13 %%% z_ref %%%
14 z_ref(y,1)=dlmread('output_ncar',' ',[12,0,12,0]);
15
16 %%% u_nref %%%
17 u_nref(y,1)=dlmread('output_ncar',' ',[8,0,8,0]);
18
19 cd ..
20 cd ..
21 cd wasp
22
23 %%% u_wi %%%
24 for n=1:12;
25    if sector_ref(y,1)==n
26    u_wi(y,:)=dlmread('output_wasp',' ',[n+1,0,n+1,19]);
27    end;
28 end;clear n;
29
30 cd ..
31
32 %%% potential fit WAsP %%%
33 fittingfunction1=fittype('a*u_wi^b','independent','u_wi');
34 coeff=fit(u_wi(y,:)',z,fittingfunction1);
35 fitcoeff1(y,:)=[coeff.a,coeff.b];
36 aux=[0:0.1:30];
37 fittingcurve1=coeff.a.*aux.^coeff.b;
38 clear coeff;clear fittingfunction1;
39 clc;
40
41 %%% heightclass %%%
42 for m=10:10:200;
43    if z_ref(y,1)>=m-10 & z_ref(y,1)<m;
44    heightclass(y,1)=m/10;
45    end;
46    if z_ref(y,1)>200;
47    heightclass(y,1)=21;
48    end;
49 end;
50
51 %%% u_wref %%%
```

```matlab
52  if heightclass(y,1)==1 | heightclass(y,1)>20;u_wref(y,1)=(z_ref(y,1)/
        fitcoeff1(y,1))^(1/fitcoeff1(y,2));end
53  for i=2:20;
54    if heightclass(y,1)==i;
55    u_wref(y,1)=u_wi(y,i-1)+(z_ref(y,1)-z(i-1,1))*(u_wi(y,i)-u_wi(y,i-1))/(z(
        i,1)-z(i-1,1));
56    end;
57  end;
58
59  %%% u_wi/u_wref %%%
60  uadim(y,:)=u_wi(y,:)./u_wref(y,1);
61
62  %%% u %%%
63  u(y,:)=uadim(y,:).*u_nref(y,1);
64
65  %%% potential fit RESULTS %%%
66  fittingfunction2=fittype('a*u^b','independent','u');
67  coeff=fit(u(y,:)',z,fittingfunction2);
68  fitcoeff2(y,:)=[coeff.a,coeff.b];
69  fittingcurve2=coeff.a.*aux.^coeff.b;
70  clear coeff;clear fittingfunction2;%clear aux;
71
72  %%% PLOT %%%
73
74  clc;
75  cd downscaling
76  filename=strcat('downscaledprofile',num2str(y),'.pdf');
77
78  plot(aux,fittingcurve1,'r-','LineWidth',2);hold on; %%% POTENTIAL FIT %%%
79  plot(u_wi(y,:),z,'kx','LineWidth',2),hold on;
80  plot(aux,fittingcurve2,'b-','LineWidth',2);hold on; %%% POTENTIAL FIT %%%
81  plot(u(y,:),z,'ko','LineWidth',2),hold on;
82  plot([0,u_nref(y,1)],[z_ref(y,1),z_ref(y,1)],'b--','LineWidth',1),hold on;
83  plot([u_nref(y,1),u_nref(y,1)],[0,z_ref(y,1)],'b--','LineWidth',1), hold on
        ;
84  plot([0,u_wref(y,1)],[z_ref(y,1),z_ref(y,1)],'r--','LineWidth',1),hold on;
85  plot([u_wref(y,1),u_wref(y,1)],[0,z_ref(y,1)],'r--','LineWidth',1), ...
86  title(datencar), ...
87  legend('WAsP (fit)','WAsP (points)','Downscaled (fit)', 'Downscaled (points
        )'), ...
88  options={'interpreter','latex','Fontsize',12}; ...
89  xlabel('$u (m/s)$',options{:}),ylabel('$z(m)$',options{:}), ...
90  set(gca,'XLim',[0,max(u_nref(y,1)+3,u_wref(y,1)+3)],'YLim',[0,z_ref(y,1)
        +100]), ...
91  set(gca,'FontSize',12,'FontName','Times'), ...
92  saveas(gcf,filename);hold off;
93
94  cd ..
95  end;
```

As mentioned in the discussion on how to determine the reference height, a little modification of the present code can be introduced in order to allow the user deciding z_{ref} arbitrarily. For this, lines from 19 to 21 concerning the computation of such parameter, have to be replaced by the following lines:

```
1  %%% z_ref %%%
2  z_ncar=dlmread('output_ncar',' ',[12,0,12,17-firstpoint]);
3  z_difference=abs(z_ncar-arbitrary_z_ref);[mindif,minpoint]=min(z_difference
      );
4  z_ref(y,1)=dlmread('output_ncar',' ',[12,minpoint-1,12,minpoint-1]);
```

And, of course, the arbitrary reference height must be defined (in meters) as variable `arbitrary_z_ref` in the code before line 19. It can also be added the following line in order to ask the user for z_{ref} when he/she runs the application:

```
1  %%% z_ref %%%
2  arbitrary_z_ref=input('Insert arbitrary reference height (m): ')
```

validation.m

```
1  %%% VALIDATION %%%
2
3  %%load observations %%%
4  cd ..
5  cd observations
6  u_obs=dlmread('observations','\t',[0 0 7 0]);
7  sector_obs=dlmread('observations','\t',[0 1 7 1]);
8  cd ..
9
10 %%% computed velocity at hub height %%%
11 hub=input('Met. Stat. mast height (m) − note that by default is generally
       10m: ');
12
13 clc;
14
15 for p=1:8;
16 u_ref(p,1)=(hub./fitcoeff2(p,1))^(1/fitcoeff2(p,2));
17 end;
18
19 %%% PLOT %%%
20
21 cd validation
22
23 %%% sectors (single) %%%
24 for t=1:8;
25
26 %r=max(u_ref(t,1),u_obs(t,1));
27 %x=−r:0.005:r;
28 %y=sqrt((r^2)−x.^2);
29 %z=−sqrt((r^2)−x.^2);
30
31 %%% direction computed %%%
32 if sector_ref(t,1)==1;dir_c=90;end;
33 if sector_ref(t,1)==2;dir_c=60;end;
34 if sector_ref(t,1)==3;dir_c=30;end;
35 if sector_ref(t,1)==4;dir_c=00;end;
36 if sector_ref(t,1)==5;dir_c=330;end;
37 if sector_ref(t,1)==6;dir_c=300;end;
38 if sector_ref(t,1)==7;dir_c=270;end;
39 if sector_ref(t,1)==8;dir_c=240;end;
40 if sector_ref(t,1)==9;dir_c=210;end;
41 if sector_ref(t,1)==10;dir_c=180;end;
42 if sector_ref(t,1)==11;dir_c=150;end;
43 if sector_ref(t,1)==12;dir_c=120;end;
44
45 dir_comp(t,1)=dir_c;
46
47 %%% direction observed %%%
48 if sector_obs(t,1)==1;dir_o=90;end;
49 if sector_obs(t,1)==2;dir_o=60;end;
50 if sector_obs(t,1)==3;dir_o=30;end;
```

```matlab
51  if  sector_obs(t,1)==4;dir_o=00;end;
52  if  sector_obs(t,1)==5;dir_o=330;end;
53  if  sector_obs(t,1)==6;dir_o=300;end;
54  if  sector_obs(t,1)==7;dir_o=270;end;
55  if  sector_obs(t,1)==8;dir_o=240;end;
56  if  sector_obs(t,1)==9;dir_o=210;end;
57  if  sector_obs(t,1)==10;dir_o=180;end;
58  if  sector_obs(t,1)==11;dir_o=150;end;
59  if  sector_obs(t,1)==12;dir_o=120;end;
60
61  dir_obs(t,1)=dir_o;
62
63  u_o=u_obs(t,1)*cosd(dir_o);
64  v_o=u_obs(t,1)*sind(dir_o);
65  u_c=u_ref(t,1)*cosd(dir_c);
66  v_c=u_ref(t,1)*sind(dir_c);
67
68  %filenamevel=strcat('validation_sector',num2str(t),'.pdf');
69  %titleplotvel=strcat('Validation sectors: sector #',num2str(t));
70  %quiver(0,0,u_c,v_c,'r','LineWidth',2);hold on; %computed%
71  %quiver(0,0,u_o,v_o,'b','LineWidth',2);hold on; %observed%
72  %plot(x,y,'k-','LineWidth',1),hold on;
73  %plot(x,z,'k-','LineWidth',1),title(titleplotvel);legend('Computed','
       Observed'),options={'interpreter','latex','Fontsize',12};xlabel('u(m/s)
       ',options{:}),ylabel('$u(m/s)$',options{:}),set(gca,'XLim',[-r,r],'YLim
       ',[-r,r]),
74  %set(gca,'FontSize',12,'FontName','Times'),saveas(gcf,filenamevel);hold off
       ;
75
76  end;
77
78  %%% velocities %%%
79  aux3=1:1:8;
80
81  plot(aux3,u_obs,'b--','LineWidth',2),hold on;
82  plot(aux3,u_ref,'r-','LineWidth',2),title('Validation velocities');grid,
       legend('Observed','Computed'),...
83  options={'interpreter','latex','Fontsize',12};xlabel('$observation~no.$',
       options{:}),ylabel('$u~(m/s)$',options{:}),...
84  set(gca,'XLim',[1,8],'YLim',[0,max(max(u_obs)+1,max(u_ref)+1)]),...
85  set(gca,'FontSize',12,'FontName','Times'),saveas(gcf,'validation_velocities
       .pdf');hold off;
86
87  %%% sector %%%
88  plot(aux3,dir_obs,'--b','LineWidth',2),hold on;
89  plot(aux3,dir_comp,'-r','LineWidth',2),title('Validation direction');
       grid,legend('Observed','Computed'),...
90  options={'interpreter','latex','Fontsize',12};xlabel('$observation~no.$'
       ,...
91  options{:}),ylabel('$direction~(^o)$',options{:}),...
92  set(gca,'XLim',[1,8],'YLim',[0,360]),...
93  set(gca,'FontSize',12,'FontName','Times'),saveas(gcf,'validation_sectors.
       pdf');hold off;
```

```matlab
94
95 %clear dir_c;clear dir_o;clear filename;clear titleplot;clear aux;clear p;
       clear t;clear fitcoeff*;clear fittingcurve*;clear heightclass;clear i;
       clear k;clear m;clear message;clear options;clear p;clear r;clear
       sector;clear u_c;clear u_o;clear v_o;clear v_c;clear x;clear y;clear z;
       clear L;clear datencar;
96
97 cd ..
98
99 disp('Done! Results saved!');
```